

# A unified framework for fitting Bayesian semiparametric models to arbitrarily censored survival data, including spatially-referenced data

Haiming Zhou

Division of Statistics, Northern Illinois University  
and

Timothy Hanson

Department of Statistics, University of South Carolina

July 4, 2017

*(To appear in Journal of the American Statistical Association)*

## Abstract

A comprehensive, unified approach to modeling arbitrarily censored spatial survival data is presented for the three most commonly-used semiparametric models: proportional hazards, proportional odds, and accelerated failure time. Unlike many other approaches, all manner of censored survival times are simultaneously accommodated including uncensored, interval censored, current-status, left and right censored, and mixtures of these. Left-truncated data are also accommodated leading to models for time-dependent covariates. Both georeferenced (location exactly observed) and areally observed (location known up to a geographic unit such as a county) spatial locations are handled; formal variable selection makes model selection especially easy. Model fit is assessed with conditional Cox-Snell residual plots, and model choice is carried out via LPML and DIC. Baseline survival is modeled with a novel transformed Bernstein polynomial prior. All models are fit via a new function which calls efficient compiled C++ in the R package `spBayesSurv`. The methodology is broadly illustrated with simulations and real data applications. An important finding is that proportional odds and accelerated failure time models often fit significantly better than the commonly-used proportional hazards model. Supplementary materials are available online.

*Keywords:* Bernstein polynomial; Interval censored data; Spatial frailty models; Variable selection

# 1 Introduction

Spatial location often plays a key role in prediction, serving as a proxy for unmeasured regional characteristics such as socioeconomic status, access and quality of healthcare, pollution, etc. Spatial models use location both as a means for blocking, leading to more precisely estimated non-spatial risk factors, but also as a focal point of inference in its own right, for example to delineate regional “hot spots” or outbreaks that merit closer attention or increased resources. Literature on the spatial analysis of time-to-event data related to human health has flourished over the last decade, including data on leukemia survival (Henderson et al., 2002), infant/childhood mortality (Banerjee et al., 2003; Kneib, 2006), coronary artery bypass grafting (Hennerfeind et al., 2006), asthma (Li and Ryan, 2002; Li and Lin, 2006), breast cancer (Zhao and Hanson, 2011; Hanson et al., 2012; Zhou et al., 2015), mortality due to air pollution (Jerrett et al., 2013), colorectal cancer survival (Liu et al., 2014), smoking cessation (Pan et al., 2014), HIV/AIDS patients (Martins et al., 2016), time to tooth loss (Schnell et al., 2015), and many others. Spatial survival models have also been used in other important areas such as the study of political event processes (Darmofal, 2009), agricultural mildew outbreaks (Ojiambo and Kang, 2013), forest fires (Morin, 2014), pine trees (Li et al., 2015a), health and pharmaceutical firms (Arbia et al., 2017), and emergency service response times (Taylor, 2017) to name a few.

All twenty papers referenced above use Cox’s (Cox, 1972) proportional hazards (PH) model for inference; competing models are not considered. There are a few papers using models alternative to PH in a spatial context, e.g. Diva et al. (2008), Zhao et al. (2009), Wang et al. (2012), and Li et al. (2015b) but they tend to be limited in scope. For example, all four of these latter papers only consider areal data, do not employ variable selection or allow time-dependent covariates, and are developed for right censored data only. In general the literature is fragmented in that a method for variable selection in the PH model for non-spatial right censored data will comprise one paper; another paper may extend the PH model for fitting current status data to general interval censored data, but does not include variable

selection, spatial frailties, etc. In this paper, a broadly inclusive, comprehensive treatment of three competing, highly interpretable semiparametric survival models, PH, proportional odds (PO), and accelerated failure time (AFT), is developed and illustrated on several real and simulated data sets. This work represents the culmination of a great deal of effort tying together many disparate ideas and methodologies in the literature as well as developing an efficient approach to mixed interval censored, exactly observed, and truncated data that can be widely applied to different semiparametric models.

Model formulation consists of a parametric portion giving relative risk (PH), odds (PO), or acceleration factors (AFT) coupled with georeferenced or areal spatial frailties, and a nonparametric baseline survival function modeled as a transformed Bernstein polynomial (TBP) (Chen et al., 2014) centered at a standard parametric family: one of log-logistic, log-normal, or Weibull. Centering the baseline allows prior mass to be roughly guided by the parametric family. The resulting distribution behaves similarly to a B-spline but where knot locations are guided by the centering family, blending the merits of both parametric and nonparametric approaches. Unlike mixtures of Dirichlet processes (Antoniak, 1974), gamma processes (Kalbfleisch, 1978), and mixtures of Polya trees (Lavine, 1992), the TBP is smooth and has a finite number of parameters, yielding an explicit likelihood that allows for many immediate generalizations and efficient block-adaptive Markov chain Monte Carlo (MCMC) inference. With judicious choice of blocking and careful use of existing parametric survival model fits, the block-adaptive approach cultivated here is robust, fully automated (e.g. no “tuning” is required), is relatively fast, and has been applied to data sets of up to a million observations. Furthermore, all of the machinery developed is available in a powerful, freely-available R function `survregbayes` calling compiled C++ in the `spBayesSurv` package (Zhou and Hanson, 2017) for R. Note that although the methodology is developed for both areal and georeferenced spatial time-to-event data, non-spatial data are also accommodated. All manner of exactly observed, right censored, interval censored, and left-truncated data are accommodated, as well as mixtures of these. Left-truncation allows for the inclusion of

time-dependent covariates and spike-and-slab variable selection is also implemented. Finally, a separate function that computes a variation on the Cox-Snell residual plot allows for gross assessment of model fit. The ready availability of software to easily fit the models developed herein allows researchers to empirically compare various competing semiparametric models on their own survival data, as well as allowing comparison to other survival models in the literature.

Section 2 describes the models including the TBP, georeferenced and areal frailties, MCMC, diagnostics and model selection criteria. Three illustrative data analyses comprise Section 3. Section 4 offers simulations illustrating the quality of estimation as well as comparing to the R packages `ICBayes` (Pan et al., 2015), `bayesSurv` (Komárek and Lesaffre, 2008) and `R2BayesX` (Umlauf et al., 2015; Belitz et al., 2015). The paper is concluded in Section 5. Tests for parametric baseline, stochastic search variable selection, left-truncation, time-dependent covariates, partially linear predictors, more simulations, as well as many other details are further discussed in the online supplementary material accompanying this paper.

## 2 The Models

Subjects are observed at  $m$  distinct spatial locations  $\mathbf{s}_1, \dots, \mathbf{s}_m$ . For areally-observed outcomes, e.g. county-level, there is typically replication at each location; for georeferenced data there may or may not be replication. Let  $t_{ij}$  be the (possibly censored) survival time for subject  $j$  at location  $\mathbf{s}_i$  and  $\mathbf{x}_{ij}$  be the corresponding  $p$ -dimensional vector of covariates,  $i = 1, \dots, m, j = 1, \dots, n_i$ ; let  $n = \sum_{i=1}^m n_i$  be the total number of subjects. Assume the survival time  $t_{ij}$  lies in the interval  $(a_{ij}, b_{ij})$ ,  $0 \leq a_{ij} \leq b_{ij} \leq \infty$ . Here left censored data are of the form  $(0, b_{ij})$ , right censored  $(a_{ij}, \infty)$ , interval censored  $(a_{ij}, b_{ij})$  and uncensored values simply have  $a_{ij} = b_{ij}$ , i.e. define  $(x, x) = \{x\}$ . The event and censoring times are assumed to be independent given the observed covariates. Note that both current status data and

case 2 interval censored data (Sun, 2006), arise as particular special cases.

Spatial dependence often arises among survival outcomes due to region-specific similarities in ecological and/or social environments that are typically not measurable or omitted due to confidentiality concerns. To incorporate such spatial dependence, a traditional way is to introduce random effects (frailties)  $v_1, \dots, v_m$  into the linear predictor of survival models. In this paper we consider three commonly-used semiparametric models: AFT, PH, and PO. Given spatially-varying frailties  $v_1, \dots, v_m$ , regression effects  $\boldsymbol{\beta} = (\beta_1, \dots, \beta_p)'$ , and baseline survival  $S_0(\cdot)$  with density  $f_0(\cdot)$  corresponding to  $\mathbf{x}_{ij} = \mathbf{0}$  and  $v_i = 0$ , the AFT model has survival and density functions

$$S_{\mathbf{x}_{ij}}(t) = S_0(e^{\mathbf{x}'_{ij}\boldsymbol{\beta}+v_i}t), \quad f_{\mathbf{x}_{ij}}(t) = e^{\mathbf{x}'_{ij}\boldsymbol{\beta}+v_i} f_0(e^{\mathbf{x}'_{ij}\boldsymbol{\beta}+v_i}t), \quad (2.1)$$

while the PH model has survival and density functions

$$S_{\mathbf{x}_{ij}}(t) = S_0(t)^{e^{\mathbf{x}'_{ij}\boldsymbol{\beta}+v_i}}, \quad f_{\mathbf{x}_{ij}}(t) = e^{\mathbf{x}'_{ij}\boldsymbol{\beta}+v_i} S_0(t)^{e^{\mathbf{x}'_{ij}\boldsymbol{\beta}+v_i}-1} f_0(t), \quad (2.2)$$

and the PO model has survival and density functions

$$S_{\mathbf{x}_{ij}}(t) = \frac{e^{-\mathbf{x}'_{ij}\boldsymbol{\beta}-v_i} S_0(t)}{1 + (e^{-\mathbf{x}'_{ij}\boldsymbol{\beta}-v_i} - 1) S_0(t)}, \quad f_{\mathbf{x}_{ij}}(t) = \frac{e^{-\mathbf{x}'_{ij}\boldsymbol{\beta}-v_i} f_0(t)}{[1 + (e^{-\mathbf{x}'_{ij}\boldsymbol{\beta}-v_i} - 1) S_0(t)]^2}. \quad (2.3)$$

In semiparametric survival analysis, a wide variety of Bayesian nonparametric priors can be used to model  $S_0(\cdot)$ ; see Müller et al. (2015) and Zhou and Hanson (2015) for reviews. In this paper we consider the models (2.1), (2.2) and (2.3) with a TBP prior on  $S_0(\cdot)$ .

## 2.1 Transformed Bernstein Polynomial Prior

For a given positive integer  $J \geq 1$ , define the Bernstein polynomial of degree  $J - 1$  as a particular B-spline over  $(0, 1)$  given by

$$d(x|J, \mathbf{w}_J) = \sum_{j=1}^J w_j \delta_{j,J}(x) \equiv \sum_{j=1}^J w_j \frac{\Gamma(J+1)}{\Gamma(j)\Gamma(J-j+1)} x^{j-1} (1-x)^{J-j}, \quad (2.4)$$

where  $\mathbf{w}_J = (w_1, \dots, w_J)'$  is a vector of positive weights satisfying  $\sum_{j=1}^J w_j = 1$  and  $\delta_{j,J}(x)$  denotes a beta density with parameters  $(j, J-j+1)$ . Smooth densities with support  $(0, 1)$  can be well approximated by a Bernstein polynomial (Ghosal, 2001): if  $f(x)$  is any continuously differentiable density with support  $(0, 1)$  and bounded second derivative,  $\mathbf{w}_J$  can be chosen such that

$$\sup_{0 < x < 1} |f(x) - d(x|J, \mathbf{w}_J)| = O(J^{-1}).$$

Integrating (2.4) gives the corresponding cumulative distribution function (cdf)

$$D(x|J, \mathbf{w}_J) = \sum_{j=1}^J w_j \Delta_{j,J}(x), \quad (2.5)$$

where  $\Delta_{j,J}(x)$  is the cdf associated with  $\delta_{j,J}(x)$ . One can calculate the summands in (2.5) recursively as

$$\Delta_{j+1,J}(x) = \Delta_{j,J}(x) - \frac{\Gamma(J+1)}{\Gamma(j+1)\Gamma(J-j+1)} x^j (1-x)^{J-j}.$$

By assigning a joint prior distribution to  $(J, \mathbf{w}_J)$ , the random  $d(x|J, \mathbf{w}_J)$  in (2.4) is said to have the Bernstein polynomial (BP) prior. Petrone (1999) showed that if the prior on  $(J, \mathbf{w}_J)$  has full support, the BP prior has positive support on all continuous density functions on  $(0, 1)$ . However, for practical reasons, the degree  $J$  is often truncated to a large value, say  $\mathcal{K}$ , so that the prior has support  $\mathcal{B}_{\mathcal{K}} = \{d(x|J, \mathbf{w}_J) : J \leq \mathcal{K}\}$ . Under mild conditions, Petrone and Wasserman (2002) showed that, for a fixed  $\mathcal{K}$ , the posterior density almost

surely converges (as  $n \rightarrow \infty$ ) to a density that minimizes the Kullback-Leibler divergence of the true density against  $d(x) \in \mathcal{B}_{\mathcal{K}}$ . BP priors of lesser degree have the same support as  $\mathcal{B}_{\mathcal{K}}$  because any Bernstein polynomial can be written in terms of Bernstein polynomials of higher degree through the relationship

$$\delta_{j,J-1}(x) = \frac{J-j}{J}\delta_{j,J}(x) + \frac{j}{J}\delta_{j+1,J}(x).$$

It follows that  $d(x|J-1, \mathbf{w}_{J-1})$  can be written as  $d(x|J, \mathbf{w}_J^*)$  with a suitable choice of  $\mathbf{w}_J^*$ , so every  $d(x|J, \mathbf{w}_J)$  with  $J \leq \mathcal{K}$  belongs to  $\{d(x|\mathcal{K}, \mathbf{w}_{\mathcal{K}})\}$ . Therefore, following Chen et al. (2014) we fix  $J$  throughout, with  $J = 15$  being the software's default. This is roughly equivalent to having 15 knots in a B-spline representation of the transformed baseline survival function, described next.

Let  $\{S_{\boldsymbol{\theta}}(\cdot) : \boldsymbol{\theta} \in \Theta\}$  denote a parametric family of survival functions with support on positive reals  $\mathbb{R}^+$ . The log-logistic family  $S_{\boldsymbol{\theta}}(t) = \{1 + (e^{\theta_1}t)^{\exp(\theta_2)}\}^{-1}$  is considered in the examples in Section 3, where  $\boldsymbol{\theta} = (\theta_1, \theta_2)'$ ; Weibull and log-normal families are also included in the R package. Note that  $S_{\boldsymbol{\theta}}(t)$  always lies in the interval  $(0, 1)$  for  $0 < t < \infty$ , so a natural prior on  $S_0(\cdot)$ , termed the TBP prior, is simply

$$S_0(t) = D(S_{\boldsymbol{\theta}}(t)|J, \mathbf{w}_J) \text{ with density } f_0(t) = d(S_{\boldsymbol{\theta}}(t)|J, \mathbf{w}_J)\boldsymbol{f}_{\boldsymbol{\theta}}(t), \quad (2.6)$$

where  $\boldsymbol{f}_{\boldsymbol{\theta}}$  is the density associated with  $S_{\boldsymbol{\theta}}(\cdot)$ . Clearly, the random distribution  $S_0(\cdot)$  is centered at  $S_{\boldsymbol{\theta}}(\cdot)$ , that is,  $E[S_0(t)] = S_{\boldsymbol{\theta}}(t)$  and  $E[f_0(t)] = \boldsymbol{f}_{\boldsymbol{\theta}}(t)$ . The weight parameters  $\mathbf{w}_J$  adjust the shape of the baseline survival  $S_0(\cdot)$  relative to the centering distribution  $S_{\boldsymbol{\theta}}(\cdot)$ . This adaptability makes the TBP prior attractive in its flexibility, but also anchors the random  $S_0(\cdot)$  firmly about  $S_{\boldsymbol{\theta}}(\cdot)$ :  $w_j = 1/J$  for  $j = 1, \dots, J$  implies  $S_0(t) = S_{\boldsymbol{\theta}}(t)$  for  $t \geq 0$ . Moreover, unlike the mixture of Polya trees (Lavine, 1992) or mixture of Dirichlet process (Antoniak, 1974) priors, the TBP prior selects smooth densities, leading to efficient posterior sampling. Initially we had implemented the models using mixtures of Polya trees (and this

function is still available in the `spBayesSurv` R package with limited functionality); these models suffered poor mixing, especially for the AFT model. The TBP provided essentially the same posterior inference or better (as measured by LPML) with vastly improved MCMC mixing; see supplemental Appendix J.4.

Regarding the prior for  $\mathbf{w}_J$ , we consider a Dirichlet distribution,  $\mathbf{w}_J|J \sim \text{Dirichlet}(\alpha, \dots, \alpha)$ , where  $\alpha > 0$  acts like the precision in a Dirichlet process (Ferguson, 1973), controlling how stochastically “pliable”  $S_0(\cdot)$  is relative to  $S_\theta(\cdot)$ . Large values of  $\alpha$  indicate a strong belief that  $S_0(\cdot)$  is close to  $S_\theta(\cdot)$ : as  $\alpha \rightarrow \infty$ ,  $S_0(t) \rightarrow S_\theta(t)$  with probability 1. Smaller values of  $\alpha$  allow more pronounced deviations of  $S_0(\cdot)$  from  $S_\theta(\cdot)$ . A gamma prior on  $\alpha$  is considered:  $\alpha \sim \Gamma(a_\alpha, b_\alpha)$  where  $E(\alpha) = a_\alpha/b_\alpha$ .

## 2.2 Spatial Frailty Modeling

Spatial frailty models are usually grouped into two general settings according to their underlying data structure (Banerjee et al., 2014): *georeferenced* data, where  $\mathbf{s}_i$  varies continuously throughout a fixed study region  $\mathcal{S}$  (e.g.,  $\mathbf{s}_i$  is recorded as longitude and latitude); and *areal* data, where  $\mathcal{S}$  is partitioned into a finite number of areal units with well-defined boundaries (e.g.,  $\mathbf{s}_i$  represents a county).

### 2.2.1 Areal Data Modeling

We consider an intrinsic conditionally autoregressive (ICAR) prior (Besag, 1974) on  $\mathbf{v} = (v_1, \dots, v_m)'$ . Let  $e_{ij}$  be 1 if regions  $i$  and  $j$  are neighbors (which can be defined in various ways) and 0 otherwise; set  $e_{ii} = 0$ . Then the  $m \times m$  matrix  $\mathbf{E} = [e_{ij}]$  is called the adjacency matrix for the  $m$  regions. The ICAR prior on  $\mathbf{v}$  is defined through the set of the conditional distributions

$$v_i|\{v_j\}_{j \neq i} \sim N\left(\sum_{j=1}^m e_{ij}v_j/e_{i+}, \tau^2/e_{i+}\right), \quad i = 1, \dots, m, \quad (2.7)$$



where  $e_{i+} = \sum_{j=1}^m e_{ij}$ ,  $\tau$  is a scale parameter, and  $\tau^2/e_{i+}$  is the conditional variance. The induced prior on  $\mathbf{v}$  under ICAR is improper; the constraint  $\sum_{j=1}^m v_j = 0$  is used for identifiability (Banerjee et al., 2014). Note that we assume that every region has at least one neighbor, so the proportionality constant for the improper density of  $\mathbf{v}$  is  $(\tau^{-2})^{(m-1)/2}$  (Lavine and Hodges, 2012).

A referee has asked about the inclusion of the proper CAR prior, which is not currently supported by the software accompanying this article. The ICAR has been generally favored over its proper counterpart, the CAR prior, for several reasons. The CAR prior includes a parameter  $\kappa$  which shrinks the frailties toward zero:  $v_i|\kappa, \{v_j\}_{j \neq i} \sim N\left(\kappa \sum_{j=1}^m e_{ij}v_j/e_{i+}, \tau^2/e_{i+}\right)$ . As  $\kappa \rightarrow 1^-$  the improper ICAR results. Paciorek (2009) suggests that the shrinkage from a proper CAR is “generally unappealing” in the spatial setting; similarly Banerjee et al. (2014) question the sensibility of smoothing a spatial effect toward a proportion  $\kappa < 1$  of the mean of its neighbors. Paciorek (2009) further notes that posterior estimates of  $\kappa$  are often close to one, essentially yielding the ICAR. This is likely due to the rather modest amount of correlation the proper CAR provides unless  $\kappa \approx 1$ ; see Assunção and Krainski (2009) and Banerjee et al. (2014).

When spatial smoothing is not of interest, we consider independent and identically distributed (IID) Gaussian frailties,  $v_1, \dots, v_m \stackrel{iid}{\sim} N(0, \tau^2)$ . This is a special case of the proper CAR prior where  $\kappa = 0$ , so the software allows for either no correlation or the maximal limiting correlation of the proper CAR prior.

### 2.2.2 Georeferenced Data Modeling

For georeferenced data, it is commonly assumed that  $v_i = v(\mathbf{s}_i)$  arises from a Gaussian random field (GRF)  $\{v(\mathbf{s}), \mathbf{s} \in \mathcal{S}\}$  such that  $\mathbf{v} = (v_1, \dots, v_m)$  follows a multivariate Gaussian distribution as  $\mathbf{v} \sim N_m(\mathbf{0}, \tau^2 \mathbf{R})$ , where  $\tau^2$  measures the amount of spatial variation across locations and the  $(i, j)$  element of  $\mathbf{R}$  is modeled as  $\mathbf{R}[i, j] = \rho(\mathbf{s}_i, \mathbf{s}_j)$ , where  $\rho(\cdot, \cdot)$  is a correlation function controlling the spatial dependence of  $v(\mathbf{s})$ . In this paper, we consider

the powered exponential correlation function  $\rho(\mathbf{s}, \mathbf{s}') = \rho(\mathbf{s}, \mathbf{s}'; \phi) = \exp\{-(\phi\|\mathbf{s} - \mathbf{s}'\|)^\nu\}$ , where  $\phi > 0$  is a range parameter controlling the spatial decay over distance,  $\nu \in (0, 2]$  is a shape parameter, and  $\|\mathbf{s} - \mathbf{s}'\|$  is the distance (e.g., Euclidean, great-circle) between  $\mathbf{s}$  and  $\mathbf{s}'$ . Note that  $\phi \rightarrow \infty$  gives the IID Gaussian prior described in Section 2.2.1 as a special case. Similar to ICAR, the conditional prior is given by

$$v_i | \{v_j\}_{j \neq i} \sim N \left( - \sum_{\{j: j \neq i\}} p_{ij} v_j / p_{ii}, \tau^2 / p_{ii} \right), \quad i = 1, \dots, m, \quad (2.8)$$

where  $p_{ij}$  is the  $(i, j)$  element of  $\mathbf{R}^{-1}$ .

As  $m$  increases evaluating  $\mathbf{R}^{-1}$  from  $\mathbf{R}$  becomes computationally impractical. Various approaches have been developed to overcome this computational issue such as process convolutions (Higdon, 2002), fixed rank kriging (Cressie and Johannesson, 2008), predictive process models (Banerjee et al., 2008), sparse approximations (Kaufman et al., 2008), and the full-scale approximation (Sang and Huang, 2012). We consider the full-scale approximation (FSA) as an option when fitting models in the accompanying R software due to its capability of capturing both large- and small-scale spatial dependence; see supplementary Appendix B for a brief introduction.

The FSA was arrived at after a number of lengthy, unsuccessful attempts at using other approximations. BayesX (Belitz et al., 2015) uses what have been termed “Matérn splines,” first introduced in an applied context by Kammann and Wand (2003). Several authors have used this approach including Kneib (2006), Hennerfeind et al. (2006), and Kneib and Fahrmeir (2007). This approximation was termed a “predictive process” and given a more formal treatment by Banerjee et al. (2008). In our experience, the predictive process tends to give biased regression effects and prediction when the rank (i.e. the number of knots) was chosen too low; the problem worsened with no replication and/or when spatial correlation was high. The FSA fixes the predictive process by adding tapering to the “residual” process. We have been able to successfully analyze data with several thousand georeferenced spatial

locations via MCMC using the FSA option with little to no artificial bias in parameter estimation and consistently good predictive ability.

Choices alternative to the powered exponential such as the spherical and Matérn correlation functions may be of interest, however the current package only supports the powered exponential correlation with pre-specified  $\nu$ . This choice has proven to be adequate across many simulated data sets and is partially borne from our experience with very weakly identified parameters in “too flexible” correlation structures. Initially we used the Matérn but moved to the powered exponential when Matérn parameters would invariably have very poor MCMC mixing and biased estimates in all but very large samples. Note that the exponential correlation function, also a special case of Matérn, is given by  $\nu = 1$  yielding continuous but not differentiable sample paths. Gaussian correlation, a limiting case of Matérn, is given by  $\nu = 2$ , providing (infinitely) differentiable sample paths.

BayesX and R-INLA (Martins et al., 2013) both include the Matérn correlation function  $\rho(\mathbf{s}, \mathbf{s}'; \phi) = [2^{\nu-1}\Gamma(\nu)]^{-1}(\phi\|\mathbf{s} - \mathbf{s}'\|)^{\nu}\mathcal{K}_{\nu}(\phi\|\mathbf{s} - \mathbf{s}'\|)$  where  $\mathcal{K}_{\nu}$  is the modified Bessel function of order  $\nu$ . Noting weakly identified Matérn parameters, BayesX requires the user to fix one of  $\nu \in \{0.5, 1.5, 2.5, 3.5\}$  ( $\nu = 0.5$  gives exponential correlation;  $\nu \rightarrow \infty$  gives Gaussian) and fixes  $\phi^{-1}$  at  $\hat{\phi}^{-1} = \max_{i,j} \|\mathbf{s}_i - \mathbf{s}_j\|/c$  with  $c$  chosen so the correlation between the two farthest locations is small, e.g. 0.001. R-INLA requires the user to fix one of  $\nu \in \{1.5, 2.5, 3.5\}$  but allows the range parameter  $\phi$  to be estimated from the data. So the approach of BayesX fixes both parameters of the Matérn correlation and R-INLA allows the range  $\phi$  to be random (as do we).

### 2.3 Likelihood Construction and MCMC

Let  $\mathcal{D} = \{(a_{ij}, b_{ij}, \mathbf{x}_{ij}, \mathbf{s}_i); i = 1, \dots, m, j = 1, \dots, n_i\}$  be the observed data. Assume  $t_{ij} \sim S_{\mathbf{x}_{ij}}(t)$  following one of (2.1), (2.2), or (2.3) with the TBP prior on  $S_0(t)$  defined in (2.6),

and  $\mathbf{v}$  following (2.7) or (2.8). The likelihood for  $(\mathbf{w}_J, \boldsymbol{\theta}, \boldsymbol{\beta}, \mathbf{v})$  is

$$L(\mathbf{w}_J, \boldsymbol{\theta}, \boldsymbol{\beta}, \mathbf{v}) = \prod_{i=1}^m \prod_{j=1}^{n_i} [S_{\mathbf{x}_{ij}}(a_{ij}) - S_{\mathbf{x}_{ij}}(b_{ij})]^{I\{a_{ij} < b_{ij}\}} f_{\mathbf{x}_{ij}}(a_{ij})^{I\{a_{ij} = b_{ij}\}}. \quad (2.9)$$

MCMC is carried out through an empirical Bayes approach coupled with adaptive Metropolis samplers (Haario et al., 2001). The posterior density is

$$p(\mathbf{w}_J, \boldsymbol{\theta}, \boldsymbol{\beta}, \mathbf{v}, \alpha, \tau^2, \phi | \mathcal{D}) \propto L(\mathbf{w}_J, \boldsymbol{\theta}, \boldsymbol{\beta}, \mathbf{v}) p(\mathbf{w}_J | \alpha) p(\alpha) p(\boldsymbol{\theta}) p(\boldsymbol{\beta}) p(\mathbf{v} | \tau^2) p(\tau^2) p(\phi),$$

where each  $p(\cdot)$  represents a prior density, and  $p(\phi)$  is only included for georeferenced data. Assume  $\boldsymbol{\theta} \sim N_2(\boldsymbol{\theta}_0, \mathbf{V}_0)$ ,  $\boldsymbol{\beta} \sim N_p(\boldsymbol{\beta}_0, \mathbf{W}_0)$ ,  $\alpha \sim \Gamma(a_\alpha, b_\alpha)$ ,  $\tau^{-2} \sim \Gamma(a_\tau, b_\tau)$  and  $\phi \sim \Gamma(a_\phi, b_\phi)$ .

Recall that  $w_j = 1/J$  implies the underlying parametric model with  $S_0(t) = S_{\boldsymbol{\theta}}(t)$ . Thus, the parametric model provides good starting values for the TBP survival model. Let  $\hat{\boldsymbol{\theta}}$  and  $\hat{\boldsymbol{\beta}}$  denote the parametric estimates of  $\boldsymbol{\theta}$  and  $\boldsymbol{\beta}$ , and let  $\hat{\mathbf{V}}$  and  $\hat{\mathbf{W}}$  denote their estimated covariance matrices, respectively. Set  $\mathbf{z}_{J-1} = (z_1, \dots, z_{J-1})'$  with  $z_j = \log(w_j) - \log(w_J)$ . The  $\boldsymbol{\beta}$ ,  $\boldsymbol{\theta}$ ,  $\mathbf{z}_{J-1}$ ,  $\alpha$  and  $\phi$  are all updated using adaptive Metropolis samplers, where the initial proposal variance is  $\hat{\mathbf{W}}$  for  $\boldsymbol{\beta}$ ,  $\hat{\mathbf{V}}$  for  $\boldsymbol{\theta}$ ,  $0.16\mathbf{I}_{J-1}$  for  $\mathbf{z}_{J-1}$  and 0.16 for  $\alpha$  and  $\phi$ . Each frailty term  $v_i$  is updated via Metropolis-Hastings, with proposal variance as the conditional prior variance of  $v_i | \{v_j\}_{j \neq i}$ ;  $\tau^{-2}$  is updated via a Gibbs step from its full conditional. A complete description and derivation of the updating steps are in supplementary Appendix A. To determine the running length of an MCMC run, one may first run a short chain without thinning, then use R packages such as `coda` (Plummer et al., 2006) and `mcmcse` (Flegal et al., 2016) for convergence diagnosis and effective sample size calculations.

Regarding the default choice for the hyperparameters, when variable selection is not implemented (see Appendix E in the online supplementary material) we set  $\boldsymbol{\beta}_0 = \mathbf{0}$ ,  $\mathbf{W}_0 = 10^{10}\mathbf{I}_p$ ,  $\boldsymbol{\theta}_0 = \hat{\boldsymbol{\theta}}$ ,  $\mathbf{V}_0 = 10\hat{\mathbf{V}}$ ,  $a_\alpha = b_\alpha = 1$ , and  $a_\tau = b_\tau = .001$ . Note here we assume a somewhat informative prior on  $\boldsymbol{\theta}$  to obviate confounding between  $\boldsymbol{\theta}$  and  $\mathbf{w}_J$ . For georeferenced data, we set  $a_\phi = 2$  and  $b_\phi = (a_\phi - 1)/\phi_0$  so that the prior of  $\phi$  has mode at  $\phi_0$ , where  $\phi_0$

satisfies  $\rho(\mathbf{s}', \mathbf{s}''; \phi_0) = 0.001$  with  $\|\mathbf{s}' - \mathbf{s}''\| = \max_{i,j} \|\mathbf{s}_i - \mathbf{s}_j\|$ . Note that Kneib and Fahrmeir (2007) simply fix  $\phi$  at  $\phi_0$ , while we allow  $\phi$  to be random around  $\phi_0$ .

## 2.4 Model Diagnostics and Comparison

For model diagnostics, a general residual defined in Cox and Snell (1968) has been widely used in a variety of regression settings. Define  $r(t_{ij}) = -\log S_{\mathbf{x}_{ij}}(t_{ij})$  for  $i = 1, \dots, m$ ,  $j = 1, \dots, n_i$ , then  $r(t_{ij})$ , given  $S_{\mathbf{x}_{ij}}(\cdot)$ , has a standard exponential distribution. Therefore, if the model is “correct,” and under arbitrary censoring, the pairs  $\{r(a_{ij}), r(b_{ij})\}$  are approximately a random arbitrarily censored sample from an  $\text{Exp}(1)$  distribution, and the estimated (Turnbull, 1974) cumulative hazard plot should be approximately straight with slope 1. Uncertainty in the plot is assessed through several cumulative hazards based on a random sample from  $[\mathbf{w}_J, \boldsymbol{\theta}, \boldsymbol{\beta}, \mathbf{v} | \mathcal{D}]$ . This is in contrast to typical Cox-Snell plots which only use point estimates.

Several researchers have pointed out that Cox-Snell residuals are conservative in that they may be straight even under quite large departures from the model (Baltazar-Aban and Pena, 1995; O’Quigley and Xu, 2005). In this case, model criteria will be more informative. We consider two popular model choice criteria: the deviance information criterion (DIC) (Spiegelhalter et al., 2002) and the log pseudo marginal likelihood (LPML) (Geisser and Eddy, 1979), where DIC (smaller is better) places emphasis on the relative quality of model fitting and LPML (larger is better) focuses on the predictive performance. Both criteria are readily computed from the MCMC output; see supplemental Appendix C for more details.

## 3 Real Data Applications

### 3.1 Loblolly Pine Survival Data

Loblolly pine is the most commercially important timber species in the Southeastern United States; estimating loblolly survival is crucial to forestry research. The dataset used in this

section consists of 45,525 loblolly pine trees at  $m = 168$  distinct sites, which were established in 1980-1981 and monitored annually until 2001-2002. During the 21-year follow-up, 5,379 trees died; the rest survived until the last follow-up and are treated as right censored. It is of interest to investigate the association between loblolly pine survival and several important risk factors after adjusting for spatial dependence among different sites. The risk factors considered include two time-independent variables, treatment and physiographic region, and three time-dependent variables—diameter at breast height, tree height and crown class—which were repeatedly measured every 3 years. Supplementary Table S6 presents some baseline characteristics for the trees.

Li et al. (2015a) fitted a semiparametric PH model with several georeferenced spatial frailty specifications. However, they showed that the PH assumption does not hold very well for treatment and physiographic region. To investigate whether the AFT or PO provides better fit, we fit each of the AFT, PH and PO models with GRF frailties to the data using the same covariates as those in Li et al. (2015a); the log-logistic centering distribution was used throughout. Here  $\nu = 1$  was fixed giving the exponential correlation function. To better investigate the spatial frailty effect, we also fit each model with IID Gaussian frailties and non-frailty models. For each MCMC run we retained 2,000 scans thinned from 50,000 after a burn-in period of 10,000 iterations. Figure 1 reports the Cox-Snell residual plots under the three GRF frailty models, where we see that the PH model severely deviates from the 45 degree line, and the AFT fits the data much better than the PH and PO. Table 1 compares all fitted models using the LPML and DIC criteria, where we can see that the AFT always outperforms the PH and PO regardless of the frailty assumptions. Under all three models, incorporating IID frailties significantly improves the goodness of fit over the non-frailty model. Some goodness of fit improvement for the GRF over the IID occurs under the AFT, but this does not happen under the PH and PO, indicating that adding spatially structured frailties can deteriorate the model if the overarching model assumption is violated.

Table 2 gives covariate effects under the AFT models. Coefficient estimates under the

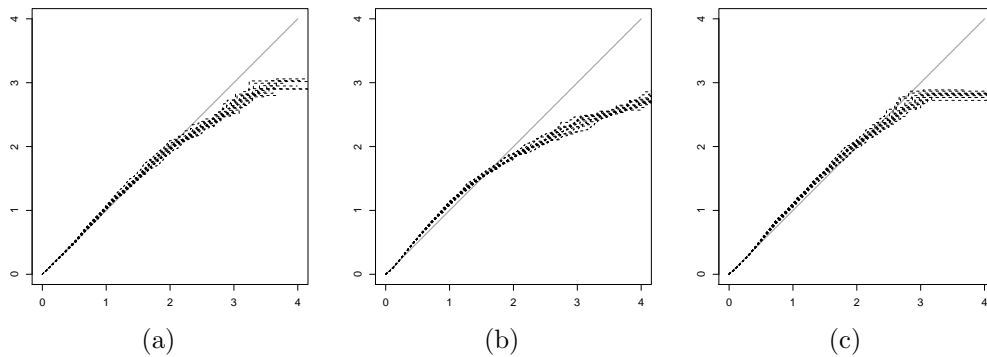


Figure 1: Loblolly pine data. Cox-Snell residual plots under AFT (panel a), PH (panel b) and PO (panel c) with GRF frailties.

Table 1: Loblolly pine data. Model comparison.

		AFT	PH	PO
GRF frailty	LPML	-23,812	-23,991	-23,882
	DIC	47,611	47,971	47,767
IID frailty	LPML	-23,832	-23,966	-23,865
	DIC	47,648	47,897	47,731
Non-frailty	LPML	-25,447	-25,508	-25,549
	DIC	50,893	51,015	51,099

Table 2: Loblolly pine data. Posterior means (95% credible intervals) of fixed effects  $\beta$  from fitting the AFT model with different frailty settings.

	Non-frailty	IID frailty	GRF frailty
DBH	-0.233(-0.255,-0.212)	-0.127(-0.144,-0.111)	-0.126(-0.142,-0.110)
TH	0.027(0.024,0.030)	-0.012(-0.015,-0.010)	-0.011(-0.014,-0.009)
treat2	-0.521(-0.583,-0.466)	-0.381(-0.423,-0.339)	-0.388(-0.431,-0.349)
treat3	-0.719(-0.798,-0.641)	-0.529(-0.589,-0.473)	-0.544(-0.601,-0.495)
PhyReg2	-0.302(-0.367,-0.241)	-0.362(-0.514,-0.198)	-0.390(-0.594,-0.201)
PhyReg3	-0.007(-0.110,0.099)	-0.254(-0.530,0.050)	-0.260(-0.511,0.014)
C2	0.097(0.028,0.169)	0.031(-0.023,0.078)	0.044(-0.002,0.097)
C3	0.835(0.747,0.923)	0.401(0.331,0.465)	0.430(0.375,0.491)
C4	1.919(1.799,2.029)	1.040(0.951,1.128)	1.101(1.018,1.194)
treat2:PhyReg2	0.146(0.041,0.244)	0.118(0.053,0.190)	0.105(0.046,0.168)
treat3:PhyReg2	0.372(0.246,0.503)	0.255(0.169,0.349)	0.246(0.162,0.332)
treat2:PhyReg3	-0.404(-0.625,-0.197)	-0.220(-0.374,-0.072)	-0.216(-0.368,-0.064)
treat3:PhyReg3	0.109(-0.129,0.325)	0.110(-0.067,0.267)	0.125(-0.037,0.286)
$\tau^2$		0.318(0.248,0.402)	0.350(0.270,0.457)
$\phi$			0.274(0.165,0.434)

model with frailties (IID or GRF) have changed significantly from those under the non-frailty model. For example, the effect of total tree height on tree survival is reversed when the model is fit with frailties. This indicates that shorter trees are associated with longer survival rates when averaged over spatial location; however taller trees have better survival rates than shorter adjusting for location. Thus a type of ‘‘Simpson’s paradox’’ occurs with space being confounded with tree height in some fashion.

We next interpret the results under the AFT model for time-dependent covariates (Prentice and Kalbfleisch, 1979) with GRF frailties, as it outperforms all other models. Table 2 shows all covariates are significant risk factors for loblolly pine survival. For example, the mean or median survival time will increase by a factor  $e^{0.126} = 1.134$  for every 1 cm increase in diameter at breast height, holding other covariates and the frailty constant. Hanson et al. (2009) note that this interpretation holds for mean or median *residual life* as well, which is of greater interest in medical contexts when choosing a course of treatment. Significant interaction effects are present between treatment and physiographic region; Figure 2 presents the survival curves for the treatment effect under different physiographic regions. The thin-



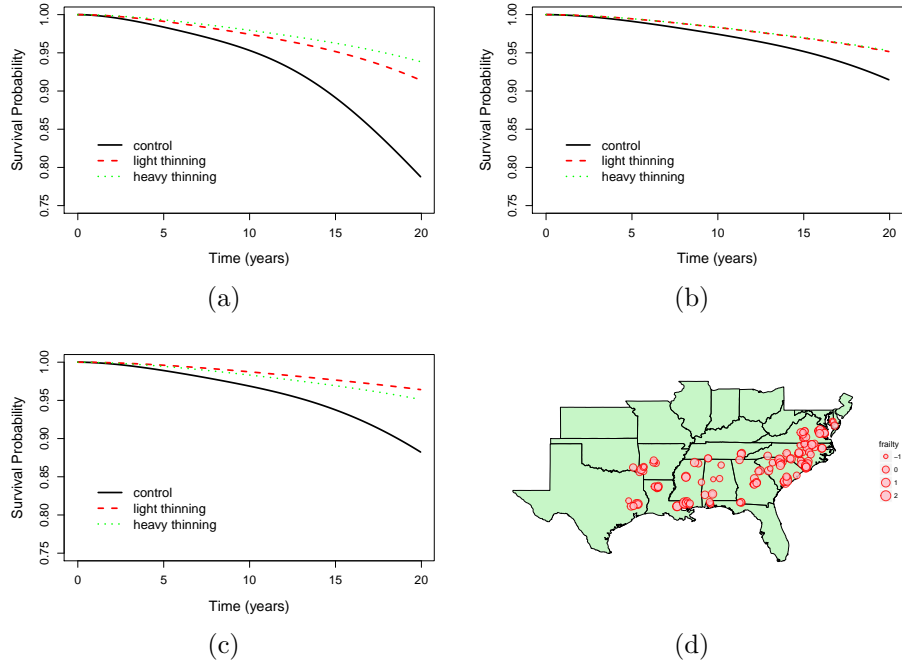


Figure 2: Loblolly pine data. Survival curves for treatment effect under coastal (panel a), Piedmont (panel b), and other (panel c) regions. The posterior means of spatial frailties for each location are mapped in panel d.

ning treatment has the largest effect on survival rates in coastal regions, while for Piedmont regions, heavy thinning is required to improve survival rates. The posterior means of spatial frailties for each location are also mapped in Figure 2, where we do not see a clear spatial pattern, implying that the spatial dependence may not be very strong for these data. To further confirm this, the posterior mean of the spatial range parameter  $\phi$  is 0.274 km. Note that 99% of the pairwise distances among the 168 locations are greater than 9.93 km, that is, 99% of the pairwise correlations are lower than  $1 - e^{-0.274 \times 9.93} \approx 0.066$ .

### 3.2 The Signal Tandmobiel Study

Oral health data collected from the Signal Tandmobiel study are next considered, available in the R package `bayesSurv`; a description of the data can be found in Komárek and Lesaffre (2009). It is of interest to investigate the impact of gender (1 = girl, 0 = boy), `dmf` (1, if the predecessor of the permanent first premolar was decayed, missing due to caries or filled,

Table 3: The Signal Tandmobiel study. Posterior means (95% credible intervals) of fixed effects from fitting the AFT, PH and PO models with IID frailties. The LPML and DIC are also shown for each model.

	AFT (LPML: -15125) (DIC: 29067)	PH (LPML: -15124) (DIC: 30045)	PO (LPML: -15503) (DIC: 30596)
gender	0.045(0.038,0.053)	1.034(0.884,1.191)	1.433(1.206,1.667)
dmf	0.031(0.026,0.036)	0.799(0.690,0.908)	1.424(1.264,1.573)
tooth	0.020(0.017,0.022)	0.408(0.341,0.472)	0.594(0.496,0.694)
dmf:tooth	-0.018(-0.022,-0.014)	-0.478(-0.578,-0.378)	-0.770(-0.921,-0.625)
gender:dmf	-0.009(-0.015,-0.003)	-0.258(-0.401,-0.126)	-0.470(-0.674,-0.260)
$\tau^2$	0.010(0.009, 0.010)	4.619(4.326, 4.918)	9.261(8.679, 9.885)

0, if the predecessor was sound), and tooth location (1 = mandibular, 0 = maxillary) on the emergence time of each of the four permanent first premolar (teeth 14, 24, 34, 44). The data set consists of 4,430 children with four tooth emergence times recorded for each child, yielding a sample size of  $n = 17,594$ . The emergence times are interval censored due to annual examinations. Komárek and Lesaffre (2009) fit an IID frailty AFT model for taking into account the dependency between emergence times within each child. Although their models allow for a nonparametric frailty density, their Figure 6 shows a remarkably Gaussian-shaped estimate. Each of the AFT, PH and PO models with IID Gaussian frailties were fit to the data using the same covariates as the Model S in (Komárek and Lesaffre, 2009, Table 4), giving LPML values -15125, -15124, and -15503, respectively. Thus, the PH and AFT models perform similarly and both outperform the PO in terms of predictive performance; however, the AFT model fits these data better than the PH according to DIC. Cox-Snell residual plots (not shown) also slightly favor AFT. Table 3 reports the fixed effects and frailty variances under each model, from which we see that the effect of dmf is different for boys and girls, and it is also different for mandibular and maxillary teeth.

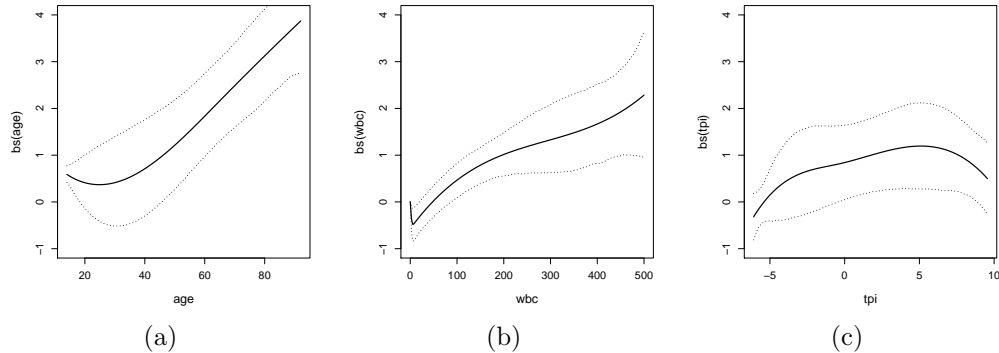


Figure 3: Leukemia data. Posterior mean estimates (solid lines) for the effects of age (panel a), wbc (panel b) and tpi (panel c), together with 95% credible intervals (dotted lines).

### 3.3 Leukemia Data

Finally, a dataset on the survival of acute myeloid leukemia in  $n = 1,043$  patients is considered, available in the package `spBayesSurv`. It is of interest to investigate possible spatial variation in survival after accounting for known subject-specific prognostic factors, which include age, sex, white blood cell count (wbc) at diagnosis, and the Townsend score (tpi) for which higher values indicates less affluent areas. There are  $m = 24$  administrative districts and each one forms a spatial cluster (Henderson et al., 2002, Figure 1). Henderson et al. (2002) fitted a multivariate gamma frailty PH model with linear predictors. Here we fit each of the PH, AFT and PO models with ICAR frailties to see whether the AFT or PO model provides better fit. To allow for non-linear effects of continuous predictors, we consider partially linear age, wbc and tpi as described in supplementary Appendix G.

The LPML values for the PH, AFT and PO models are -5946, -5945, and -5919, respectively. The PO model significantly outperforms others from a predictive point of view with a pseudo Bayes factor on the order of  $10^{10}$  relative to PH and AFT. Figure 3 presents the estimated effects of age, wbc and tpi under the PO model. The Bayes Factors for testing the linearity of age, wbc and tpi are 0.13, 0.04 and 0.01, respectively; non-linear effects are not needed.

## 4 Simulations

Extensive simulations were carried out to evaluate the proposed MCMC algorithms (implemented in `spBayesSurv`) under the three survival models with arbitrarily censored spatial data. The proposed methodology is then compared to monotone splines (Lin et al., 2015) as implemented in `ICBayes` for PH and PO, Bayesian G-splines (Komarek, 2006) implemented in `bayesSurv` for AFT, and geoaddivitive PH modeling (Hennerfeind et al., 2006) implemented in `R2BayesX`. Additional simulations for georeferenced data and variable selection are available in supplementary Appendixes J.2 and J.3.

### 4.1 Simulation I: Areal Data

For each of AFT, PH and PO, data were generated from (2.1), (2.2) and (2.3), respectively, where covariates  $\mathbf{x}_{ij} = (x_{ij1}, x_{ij2})'$  were sampled  $x_{ij1} \stackrel{iid}{\sim} \text{Bernoulli}(0.5)$  independent of  $x_{ij2} \stackrel{iid}{\sim} N(0, 1)$  for  $i = 1, \dots, 37$  and  $j = 1, \dots, 20$  ( $n = 740$ ), regression effects set to  $\boldsymbol{\beta} = (\beta_1, \beta_2)' = (1, 1)'$ , the baseline survival distribution  $S_0(t) = 1 - 0.5[\Phi(2(\log t + 1)) + \Phi(2(\log t - 1))]$  was bimodal, and  $\mathbf{v}$  followed the ICAR model (2.7) with  $\tau^2 = 1$  and  $\mathbf{E}$  equaling the Nigeria adjacency matrix used in the childhood mortality data analysis of Kneib (2006). Half the data were right censored (including uncensored survival times) and half interval censored. The times at which survival was right censored were independently simulated from a `Uniform(2, 6)` distribution. For interval censoring, each subject was assumed to have  $N$  observation times,  $O_1, O_2, \dots, O_N$ , where  $(N - 1) \sim \text{Poisson}(2)$  and  $(O_k - O_{k-1})|N \stackrel{iid}{\sim} \text{Exp}(1)$  with  $O_0 = 0$ ,  $k = 1, \dots, N$ . The censoring interval endpoints are the two adjacent observation times among  $\{0, O_1, \dots, O_N, \infty\}$  that include the true survival time. The final data yield around 20% right censored, 40% uncensored, 25% left censored and 15% interval censored. For each model, 500 Monte Carlo (MC) replicate data sets were generated. Models were fit using the default priors introduced in Section 2.3. For each MCMC run, 5,000 scans were thinned from 50,000 after a burn-in period of 10,000 iterations; convergence diagnostics deemed this

Table 4: Simulation I: average bias (BIAS) and posterior standard deviation (PSD) of each point estimate, standard deviation (across 500 MC replicates) of the point estimate (SD-Est), coverage probability (CP) for the 95% credible interval, and effective sample size (ESS) out of 5,000 with thinning=10 for each point estimate.

Model	Parameter	BIAS	PSD	SD-Est	CP	ESS
AFT	$\beta_1 = 1$	0.000	0.067	0.062	0.960	3194
	$\beta_2 = 1$	0.002	0.036	0.034	0.960	2992
	$\tau^2 = 1$	0.015	0.311	0.298	0.942	4561
PH	$\beta_1 = 1$	-0.021	0.100	0.099	0.936	3024
	$\beta_2 = 1$	-0.014	0.061	0.060	0.944	2095
	$\tau^2 = 1$	-0.039	0.352	0.319	0.950	3478
PO	$\beta_1 = 1$	0.012	0.151	0.152	0.940	3672
	$\beta_2 = 1$	0.008	0.083	0.086	0.944	2822
	$\tau^2 = 1$	-0.008	0.465	0.448	0.924	2451

more than adequate.

Table 4 summarizes the results for regression parameters  $\beta$  and the ICAR variance  $\tau^2$ , including the averaged bias (BIAS) and posterior standard deviation (PSD) of each point estimate (posterior mean for  $\beta$  and median for  $\tau^2$ ), the standard deviation (across 500 MC replicates) of the point estimate (SD-Est), the coverage probability (CP) of the 95% credible interval, and average effective sample size (ESS) out of 5,000 (Sargent et al., 2000) for each point estimate. The results show that the point estimates of  $\beta$  and  $\tau^2$  are unbiased under all three models, SD-Est values are close to the corresponding PSDs, the CP values are close to the nominal 95% level, and ESS values are promising. Supplementary Figure S1 presents the average across the 500 MC replicates of the fitted baseline survival functions revealing that the proposed model is capable to capture complex baseline survival curves very well.

## 4.2 Simulation II: Comparison

In this section we compare our R function `survregbayes` in the package `spBayesSurv` with R functions `ICBayes` in the package `ICBayes`, `bayessurvreg2` in the package `bayesSurv` and `bayesx` in the package `R2BayesX` in terms of mixing and computing speed. Our `survregbayes`

function can fit spatial or non-spatial PH, AFT and PO models (either no, IID, ICAR or GRF frailties) for all common types of survival (uncensored, interval censored, current status, right censored, etc.) and/or left-truncated data. In contrast, `ICBayes` fits only non-frailty PH and PO models to interval censored data (uncensored data is not supported), `bayessurvreg2` fits the AFT model (either no or IID frailties) to general interval censored data, and `bayesx` fits the PH model to right-censored data using MCMC. Data are generated from three cases: (C1) the non-frailty PH model with interval censoring, (C2) the non-frailty AFT model with arbitrary censoring, and (C3) the non-frailty PH model with right censoring, where  $\beta$  and  $S_0(\cdot)$  are the same as those used in **Simulation I**. Under each setting we generate 500 MC replicates, each with sample size  $n = 500$ . For each MCMC run, we retain 10,000 scans without thinning after a burn-in period of 10,000 iterations.

Table 5 reports the comparison results; the ESS from `survregbayes` range from 3 to 20 times as large as those using `ICBayes` and `bayessurvreg2`, indicating that the proposed MCMC algorithms are more efficient in terms of mixing. In addition, `survregbayes` is about 5 times faster than `ICBayes`, although it is much slower than `bayessurvreg2` and `bayesx`. Note that `bayessurvreg2` is almost 9 times faster than our `survregbayes`, but its ESS for  $\beta_1$  is nearly 19 times smaller than ours. That is, `bayessurvreg2` needs to take 19 times more iterates than ours to obtain the same ESS, thus tempering superior speed with much poorer MCMC mixing. In comparison with `bayesx` for right censored data, our `survregbayes` performs slightly worse in terms of both speed and mixing. This is not surprising, because our MCMC is designed for all AFT, PH and PO with all manner of censoring schemes while the MCMC in `bayesx` is tailored to PH with right censored data.

`ICBayes` stems from a burgeoning literature on fitting PO and PH models to interval censored data using a monotone spline, essentially an integrated B-spline, as the baseline cumulative hazard function. In particular Cai et al. (2011) consider a PH model for current status data; Lin and Wang (2011) consider the PO model with current status data; case 2 interval censoring is considered for PO by Wang and Lin (2011). Pan et al. (2014) consider

Table 5: Simulation II: average bias (BIAS) and posterior standard deviation (PSD) of each point estimate, standard deviation (across 500 MC replicates) of the point estimate (SD-Est), coverage probability (CP) for the 95% credible interval, average effective sample size (ESS) out of 10,000 without thinning for each point estimate, and average computing time in seconds.

Case	R function	Time	Parameter	BIAS	PSD	SD-Est	CP	ESS
C1	survregbayes	63	$\beta_1 = 1$	-0.018	0.134	0.134	0.940	1139
			$\beta_2 = 1$	-0.015	0.086	0.087	0.940	934
	ICBayes	310	$\beta_1 = 1$	-0.036	0.133	0.132	0.938	346
			$\beta_2 = 1$	-0.019	0.084	0.085	0.938	292
C2	survregbayes	54	$\beta_1 = 1$	0.000	0.075	0.074	0.950	1207
			$\beta_2 = 1$	0.002	0.041	0.040	0.952	1186
	bayessurvreg2	6	$\beta_1 = 1$	-0.002	0.072	0.075	0.936	64
			$\beta_2 = 1$	-0.001	0.039	0.040	0.934	109
C3	survregbayes	85	$\beta_1 = 1$	-0.009	0.103	0.061	0.954	1028
			$\beta_2 = 1$	-0.010	0.107	0.061	0.950	673
	bayesx	44	$\beta_1 = 1$	0.017	0.103	0.062	0.940	989
			$\beta_2 = 1$	0.014	0.111	0.064	0.952	2817

the PH model for general interval censored data with spatial CAR frailties and Lin et al. (2015) consider the same PH model with general interval censored data without frailties. Wang et al. (2016) take the E-M approach to the model of Lin et al. (2015). Among these papers Lin et al. (2015) state concerning the ICBayes function that “...our developed Gibbs sampler is easy to execute with only four steps and efficient because it does not require imputing any unobserved failure times or contain any complicated Metropolis-Hastings steps.” They further say that their approach is efficient in the sense that their approach is easy to program. However, although the Lin et al. (2015) approach does not require imputing failure times, it does require imputing as many latent Poisson variates as there are spline basis functions per observation, i.e. much more latent data than simply imputing the survival times. Furthermore, they update one regression coefficient  $\beta_j$  at a time for  $j = 1, \dots, p$  via the ARS method (Gilks and Wild, 1992), and it is well-known that any component-at-a-time sampler will suffer from poor mixing if there is strong correlation in the posterior.

The simplest way to improve mixing is through the consideration correlated proposals such as the adaptive version developed here or the iteratively weighted least squares proposal used in Hennerfeind et al. (2006). This simulation shows that adaptive block updates can dramatically outperform a Gibbs sampler with latent data, both in terms of speed and mixing. Furthermore, the monotone spline approach models the baseline cumulative hazard over the range of the observed data only; however, the AFT model maps observed data onto “baseline support” through a scale factor. The TBP prior used here includes a scale and so is applicable to all of PH, PO, and AFT, as well as accelerated hazards (which also needs a scale term), additive hazards, proportional mean residual life, and others.

## 5 Discussion

The recent surge in literature analyzing spatially correlated time-to-event data focusing on PH highlights the need for flexible, robust methodology and software to enable the ready use of other competing yet easily-interpretable survival models, spatial or not. This article provides a unified framework for considering competing models to PH, i.e. AFT and PO, including variable selection, areal or georeferenced frailties, and additive structure. The freely available `survregbayes` function allows for easy fitting of these competing models. An important aspect associated with the Bayesian nonparametric TBP – or more accurately richly parametric – formulation of the AFT, PH, and PO models presented here is that the assumption of the same flexible prior on  $S_0(\cdot)$  places these models common ground. Differences in fit and/or predictive performance can therefore be attributed to the semiparametric models only, rather than to additional possible differences in quite different nonparametric priors (e.g. gamma process vs. beta process vs. Dirichlet process mixture) or estimation methods (e.g. NPMLE vs. partial likelihood vs. sieves).

In two of the three data analyses in Section 3 a model alternative to PH was favored by the predictive LPML measure; for the dental data in Section 3.2, the AFT and PH



predictively perform about equally well and outperform PO. However, PH can be certainly be the best model choice from a predictive point of view; this is, of course, data-dependent. In additional analyses not presented here, the proposed AFT, PH and PO models were applied to spatial smoking cessation data set from the Lung Health Study carried out by Murray et al. (1998) and analyzed by Pan et al. (2014). The LPML values were -211, -206, and -206, respectively, indicating that PH and PO models predict equally well and outperform AFT; the pseudo Bayes factor comparing PH to AFT (or PO to AFT) is approximately  $e^{-206-(-211)} \approx 150$ . We also analyzed the current status lung cancer data set available in the R package `ICBayes`, analyzed by Sun (2006). The LPML values under the AFT, PH and PO are all essentially -83, respectively, indicating that there is essentially no difference on the predictive performance among the three models. This makes sense as the only covariate (treatment) was not significant:  $\beta = \mathbf{0}$  implies PH, PO, and AFT reduce to  $S_0(\cdot)$ .

## Supplementary Materials

**Appendices:** Appendix A: MCMC sampling algorithms; Appendix B: brief introduction to the full-scale approximation; Appendix C: definitions of the DIC and LPML criteria; Appendix D: testing for parametric  $S_0(\cdot)$ ; Appendix E: stochastic search variable selection; Appendix F: left-truncation and time-dependent covariates; Appendix G: partially linear predictors; Appendix H: introduction to the R function `survregbayes`; Appendix I: additional results for real data applications; Appendix J: additional simulation results. (pdf file)

**Data and Code:** Data and R code for the three analyses in Section 3. (zip file)

## References

- Antoniak, C. E. (1974). Mixtures of Dirichlet processes with applications to Bayesian non-parametric problems. *The Annals of Statistics*, 2(6):1152–1174.
- Arbia, G., Espa, G., Giuliani, D., and Micciolo (2017). A spatial analysis of health and pharmaceutical firm survival. *Journal of Applied Statistics*, 44(9):1560–1575.
- Assunção, R. and Krainski, E. (2009). Neighborhood dependence in Bayesian spatial models. *Biometrical Journal*, 51(5):851–869.
- Baltazar-Aban, I. and Pena, E. A. (1995). Properties of hazard-based residuals and implications in model diagnostics. *Journal of the American Statistical Association*, 90(429):185–197.
- Banerjee, S., Carlin, B. P., and Gelfand, A. E. (2014). *Hierarchical Modeling and Analysis for Spatial Data, Second Edition*. Chapman and Hall/CRC Press.
- Banerjee, S., Gelfand, A. E., Finley, A. O., and Sang, H. (2008). Gaussian predictive process models for large spatial data sets. *Journal of the Royal Statistical Society: Series B (Statistical Methodology)*, 70(4):825–848.
- Banerjee, S., Wall, M. M., and Carlin, B. P. (2003). Frailty modeling for spatially correlated survival data, with application to infant mortality in Minnesota. *Biostatistics*, 4(1):123–142.
- Belitz, C., Brezger, A., Klein, N., Kneib, T., Lang, S., and Umlauf, N. (2015). *BayesX - Software for Bayesian Inference in Structured Additive Regression Models*. Version 3.0. Available from <http://www.bayesx.org>.
- Besag, J. (1974). Spatial interaction and the statistical analysis of lattice systems. *Journal of the Royal Statistical Society: Series B*, 36(2):192–236.

- Cai, B., Lin, X., and Wang, L. (2011). Bayesian proportional hazards model for current status data with monotone splines. *Computational Statistics & Data Analysis*, 55(9):2644–2651.
- Chen, Y., Hanson, T., and Zhang, J. (2014). Accelerated hazards model based on parametric families generalized with Bernstein polynomials. *Biometrics*, 70(1):192–201.
- Cox, D. R. (1972). Regression models and life-tables (with discussion). *Journal of the Royal Statistical Society. Series B (Methodological)*, 34(2):187–220.
- Cox, D. R. and Snell, E. J. (1968). A general definition of residuals. *Journal of the Royal Statistical Society. Series B (Methodological)*, 30(2):248–275.
- Cressie, N. and Johannesson, G. (2008). Fixed rank kriging for very large spatial data sets. *Journal of the Royal Statistical Society: Series B (Statistical Methodology)*, 70(1):209–226.
- Darmofal, D. (2009). Bayesian spatial survival models for political event processes. *American Journal of Political Science*, 53(1):241–257.
- Diva, U., Dey, D. K., and Banerjee, S. (2008). Parametric models for spatially correlated survival data for individuals with multiple cancers. *Statistics in Medicine*, 27(12):2127–2144.
- Ferguson, T. S. (1973). A Bayesian analysis of some nonparametric problems. *The Annals of Statistics*, 1(2):209–230.
- Flegal, J. M., Hughes, J., and Vats, D. (2016). *mcmcse: Monte Carlo Standard Errors for MCMC*. Riverside, CA and Minneapolis, MN. R package version 1.2-1.
- Geisser, S. and Eddy, W. F. (1979). A predictive approach to model selection. *Journal of the American Statistical Association*, 74(365):153–160.
- Ghosal, S. (2001). Convergence rates for density estimation with Bernstein polynomials. *The Annals of Statistics*, 29(5):1264–1280.

- Gilks, W. R. and Wild, P. (1992). Adaptive rejection sampling for Gibbs sampling. *Applied Statistics*, 41(2):337–348.
- Haario, H., Saksman, E., and Tamminen, J. (2001). An adaptive Metropolis algorithm. *Bernoulli*, 7(2):223–242.
- Hanson, T., Johnson, W., and Laud, P. (2009). Semiparametric inference for survival models with step process covariates. *Canadian Journal of Statistics*, 37(1):60–79.
- Hanson, T. E., Jara, A., Zhao, L., et al. (2012). A Bayesian semiparametric temporally-stratified proportional hazards model with spatial frailties. *Bayesian Analysis*, 7(1):147–188.
- Henderson, R., Shimakura, S., and Gorst, D. (2002). Modeling spatial variation in leukemia survival data. *Journal of the American Statistical Association*, 97(460):965–972.
- Hennerfeind, A., Brezger, A., and Fahrmeir, L. (2006). Geoaddivitive survival models. *Journal of the American Statistical Association*, 101(475):1065–1075.
- Higdon, D. (2002). Space and space-time modeling using process convolutions. In *Quantitative methods for current environmental issues*, pages 37–56. Springer.
- Jerrett, M., Burnett, R. T., Beckerman, B. S., Turner, M. C., Krewski, D., Thurston, G., Martin, R. V., van Donkelaar, A., Hughes, E., Shi, Y., Gapstur, S. M., Thun, M. J., and Pope, C. A. (2013). Spatial analysis of air pollution and mortality in California. *American Journal of Respiratory and Critical Care Medicine*, 188(5):593–599.
- Kalbfleisch, J. (1978). Non-parametric Bayesian analysis of survival time data. *Journal of the Royal Statistical Society, Series B*, 40(2):214–221.
- Kammann, E. E. and Wand, M. P. (2003). Geoaddivitive models. *Applied Statistics*, 52(1):1–18.

- Kaufman, C. G., Schervish, M. J., and Nychka, D. W. (2008). Covariance tapering for likelihood-based estimation in large spatial data sets. *Journal of the American Statistical Association*, 103(484):1545–1555.
- Kneib, T. (2006). Mixed model-based inference in ge additive hazard regression for interval-censored survival times. *Computational Statistics & Data Analysis*, 51(2):777–792.
- Kneib, T. and Fahrmeir, L. (2007). A mixed model approach for ge additive hazard regression. *Scandinavian Journal of Statistics*, 34(1):207–228.
- Komarek, A. (2006). *Accelerated failure time models for multivariate interval-censored data with flexible distributional assumptions*. PhD thesis, PhD thesis, Katholieke Universiteit Leuven, Faculteit Wetenschappen.
- Komárek, A. and Lesaffre, E. (2008). Bayesian accelerated failure time model with multivariate doubly-interval-censored data and flexible distributional assumptions. *Journal of the American Statistical Association*, 103(482):523–533.
- Komárek, A. and Lesaffre, E. (2009). The regression analysis of correlated interval-censored data illustration using accelerated failure time models with flexible distributional assumptions. *Statistical Modelling*, 9(4):299–319.
- Lavine, M. (1992). Some aspects of Polya tree distributions for statistical modelling. *The Annals of Statistics*, 20(3):1222–1235.
- Lavine, M. L. and Hodges, J. S. (2012). On rigorous specification of ICAR models. *The American Statistician*, 66(1):42–49.
- Li, J., Hong, Y., Thapa, R., and Burkhart, H. E. (2015a). Survival analysis of loblolly pine trees with spatially correlated random effects. *Journal of the American Statistical Association*, 110(510):486–502.

- Li, L., Hanson, T., and Zhang, J. (2015b). Spatial extended hazard model with application to prostate cancer survival. *Biometrics*, 71(2):313–322.
- Li, Y. and Lin, X. (2006). Semiparametric normal transformation models for spatially correlated survival data. *Journal of the American Statistical Association*, 101(474):591–603.
- Li, Y. and Ryan, L. (2002). Modeling spatial survival data using semiparametric frailty models. *Biometrics*, 58(2):287–297.
- Lin, X., Cai, B., Wang, L., and Zhang, Z. (2015). A Bayesian proportional hazards model for general interval-censored data. *Lifetime Data Analysis*, 21(3):470–490.
- Lin, X. and Wang, L. (2011). Bayesian proportional odds models for analyzing current status data: Univariate, clustered, and multivariate. *Communications in Statistics-Simulation and Computation*, 40(8):1171–1181.
- Liu, Y., Sun, D., and He, C. Z. (2014). A hierarchical conditional autoregressive model for colorectal cancer survival data. *Wiley Interdisciplinary Reviews: Computational Statistics*, 6(1):37–44.
- Martins, R., Silva, G. L., and Andreozzi, V. (2016). Bayesian joint modeling of longitudinal and spatial survival AIDS data. *Statistics in Medicine*, 35(19):3368–3384.
- Martins, T. G., Simpson, D., Lindgren, F., and Rue, H. (2013). Bayesian computing with INLA: New features. *Computational Statistics & Data Analysis*, 67:68 – 83.
- Morin, A. A. (2014). A spatial analysis of forest fire survival and a marked cluster process for simulating fire load. Master’s thesis, The University of Western Ontario, London, Ontario, Canada.
- Müller, P., Quintana, F., Jara, A., and Hanson, T. (2015). *Bayesian Nonparametric Data Analysis*. Springer-Verlag: New York.

- Murray, R. P., Anthonisen, N. R., Connett, J. E., Wise, R. A., Lindgren, P. G., Greene, P. G., Nides, M. A., Group, L. H. S. R., et al. (1998). Effects of multiple attempts to quit smoking and relapses to smoking on pulmonary function. *Journal of clinical epidemiology*, 51(12):1317–1326.
- Ojiambo, P. and Kang, E. (2013). Modeling spatial frailties in survival analysis of cucurbit downy mildew epidemics. *Phytopathology*, 103(3):216–227.
- O’Quigley, J. and Xu, R. (2005). Goodness of fit in survival analysis. In *Encyclopedia of Biostatistics*. John Wiley & Sons, Ltd.
- Paciorek, C. (2009). Technical Vignette 5: Understanding intrinsic Gaussian Markov random field spatial models, including intrinsic conditional autoregressive models. Technical report, Department of Statistics, University of California, Berkeley, and Department of Biostatistics, Harvard School of Public Health. <http://www.stat.berkeley.edu/~paciorek/research/techVignettes/techVignette5.pdf>.
- Pan, C., Cai, B., Wang, L., and Lin, X. (2014). Bayesian semiparametric model for spatially correlated interval-censored survival data. *Computational Statistics & Data Analysis*, 74:198–209.
- Pan, C., Cai, B., Wang, L., and Lin, X. (2015). *ICBayes: Bayesian Semiparametric Models for Interval-Censored Data*. R package version 1.0.
- Petrone, S. (1999). Random Bernstein polynomials. *Scandinavian Journal of Statistics*, 26(3):373–393.
- Petrone, S. and Wasserman, L. (2002). Consistency of Bernstein polynomial posteriors. *Journal of the Royal Statistical Society: Series B (Statistical Methodology)*, 64(1):79–100.
- Plummer, M., Best, N., Cowles, K., and Vines, K. (2006). CODA: Convergence diagnosis and output analysis for MCMC. *Journal of the American Statistical Association*, 6(1):7–11.

- Prentice, R. L. and Kalbfleisch, J. D. (1979). Hazard rate models with covariates. *Biometrics*, 35(1):25–39.
- Sang, H. and Huang, J. Z. (2012). A full scale approximation of covariance functions for large spatial data sets. *Journal of the Royal Statistical Society: Series B (Statistical Methodology)*, 74(1):111–132.
- Sargent, D. J., Hodges, J. S., and Carlin, B. P. (2000). Structured Markov chain Monte Carlo. *Journal of Computational and Graphical Statistics*, 9(2):217–234.
- Schnell, P., Bandyopadhyay, D., Reich, B. J., and Nunn, M. (2015). A marginal cure rate proportional hazards model for spatial survival data. *Journal of the Royal Statistical Society: Series C (Applied Statistics)*, 64(4):673–691.
- Spiegelhalter, D. J., Best, N. G., Carlin, B. P., and Van Der Linde, A. (2002). Bayesian measures of model complexity and fit. *Journal of the Royal Statistical Society, Series B*, 64(4):583–639.
- Sun, J. (2006). *The Statistical Analysis of Interval-censored Failure Time Data*. Springer-Verlag New York.
- Taylor, B. M. (2017). Spatial modelling of emergency service response times. *Journal of the Royal Statistical Society: Series A (Statistics in Society)*, 180(2):433–453.
- Turnbull, B. W. (1974). Nonparametric estimation of a survivorship function with doubly censored data. *Journal of the American Statistical Association*, 69(345):169–173.
- Umlauf, N., Adler, D., Kneib, T., Lang, S., and Zeileis, A. (2015). Structured additive regression models: An R interface to BayesX. *Journal of Statistical Software*, 63(21):1–46.
- Wang, L. and Lin, X. (2011). A Bayesian approach for analyzing case 2 interval-censored data under the semiparametric proportional odds model. *Statistics & Probability Letters*, 81(7):876–883.



- Wang, L., McMahan, C. S., Hudgens, M. G., and Qureshi, Z. P. (2016). A flexible, computationally efficient method for fitting the proportional hazards model to interval-censored data. *Biometrics*, 72(1):222–231.
- Wang, S., Zhang, J., and Lawson, A. B. (2012). A Bayesian normal mixture accelerated failure time spatial model and its application to prostate cancer. *Statistical Methods in Medical Research*, <http://dx.doi.org/10.1177/0962280212466189>.
- Zhao, L. and Hanson, T. E. (2011). Spatially dependent Polya tree modeling for survival data. *Biometrics*, 67(2):391–403.
- Zhao, L., Hanson, T. E., and Carlin, B. P. (2009). Mixtures of Polya trees for flexible spatial frailty survival modelling. *Biometrika*, 96(2):263–276.
- Zhou, H. and Hanson, T. (2015). Bayesian spatial survival models. In *Nonparametric Bayesian Inference in Biostatistics*, pages 215–246. Springer.
- Zhou, H. and Hanson, T. (2017). *spBayesSurv: Bayesian Modeling and Analysis of Spatially Correlated Survival Data*. R package version 1.1.1.
- Zhou, H., Hanson, T., Jara, A., and Zhang, J. (2015). Modeling county level breast cancer survival data using a covariate-adjusted frailty proportional hazards model. *The Annals of Applied Statistics*, 9(1):43–68.

# Supplementary Materials for “A unified framework for fitting Bayesian semiparametric models to arbitrarily censored survival data, including spatially-referenced data” by Haiming Zhou and Timothy Hanson

## Appendix 0 Notation and Prior Tables

Table S1 presents the notation symbols used in the main paper and their definitions. Table S2 lists the priors for all parameters and the reasons of choosing them, where  $TBP_J(\alpha, S_\theta)$  is the TBP prior,  $ICAR(\tau^2)$  is the ICAR prior,  $GRF(\tau^2, \phi)$  is the GRF prior, and  $IID(\tau^2)$  is the IID prior.

Table S1: List of Notations.

Notation	Definition
$\alpha$	precision parameter of the TBP prior
$\boldsymbol{\beta} = (\beta_1, \dots, \beta_p)'$	$p$ -vector of regression coefficients for survival models
$\boldsymbol{\beta}_0$	mean of the normal $N_p(\boldsymbol{\beta}_0, \mathbf{W}_0)$ prior on $\boldsymbol{\beta}$
$\hat{\boldsymbol{\beta}}$	estimate of $\boldsymbol{\beta}$ under the parametric survival model with $S_0 = S_\theta$
$\delta_{j,J}(\cdot)$	beta density function with parameters $(j, J - 1 + 1)$
$\Delta_{j,J}(\cdot)$	beta cumulative distribution function with parameters $(j, J - 1 + 1)$
$\boldsymbol{\gamma} = (\gamma_1, \dots, \gamma_p)'$	latent binary variable with $\gamma_\ell = 1$ indicating the presence of the $\ell$ th covariate, $\ell = 1, \dots, p$
$\Gamma(a, b)$	gamma distribution with shape parameter $a$ and rate parameter $b$
$\boldsymbol{\theta} = (\theta_1, \theta_2)'$	parameters of the centering distribution families $S_\theta$
$\boldsymbol{\theta}_0$	mean of the normal $N_2(\boldsymbol{\theta}_0, \mathbf{V}_0)$ prior on $\boldsymbol{\theta}$
$\hat{\boldsymbol{\theta}}$	estimate of $\boldsymbol{\theta}$ under the parametric survival model with $S_0 = S_\theta$
$\nu$	powered exponential correlation function shape parameter, $\nu \in (0, 2]$
$\boldsymbol{\xi}_\ell = (\xi_{\ell 1}, \dots, \xi_{\ell K})'$	coefficients of the cubic B-spline basis functions for the $\ell$ th covariate, $\ell = 1, \dots, p$
$\rho(\cdot, \cdot)$	correlation function; arguments are two spatial locations
$\rho(\cdot, \cdot; \phi)$	correlation function indexed by the range parameter $\phi$
$\kappa$	shrinkage parameter used under the proper CAR
$\tau^2$	scale parameter under the ICAR or GRF or IID frailty prior
$\phi$	range parameter in the powered exponential correlation function
$a_{ij}, b_{ij}$	endpoints of the interval $(a_{ij}, b_{ij})$ that contains the survival time $t_{ij}$ , $i = 1, \dots, m, j = 1, \dots, n_i$
$a_\alpha, b_\alpha$	shape and rate parameters of the $\Gamma(a_\alpha, b_\alpha)$ prior on $\alpha$
$a_\tau, b_\tau$	shape and rate parameters of the $\Gamma(a_\tau, b_\tau)$ prior on $\tau^{-2}$

Table S1: List of Notations.

Notation	Definition
$a_\phi, b_\phi$	shape and rate parameters of the $\Gamma(a_\phi, b_\phi)$ prior on $\phi$
$A$	number of knots used in the FSA
$B$	number of blocks used in the FSA
$\mathbf{C}$	precision matrix of the vector of frailties $\mathbf{v} = (v_1, \dots, v_m)'$
$d(\cdot J, \mathbf{w}_J)$	density function of Bernstein polynomial
$D(\cdot J, \mathbf{w}_J)$	cdf associated with density $d(\cdot J, \mathbf{w}_J)$
$\mathbf{F}_e$	$m \times m$ diagonal matrix with the $i$ diagonal element being $e_{i+}$
$e_{ij}$	equals 1 if regions $i$ and $j$ share a common boundary and 0 otherwise, $i, j = 1, \dots, m$ ; set $e_{ii} = 0$
$e_{i+}$	number of adjacent regions for region $i$ , i.e. $e_{i+} = \sum_{j=1}^m e_{ij}$
$\mathbf{E}$	$m \times m$ adjacency matrix with the $ij$ th element equal to $e_{ij}$
$f_{\mathbf{x}_{ij}}(\cdot)$	density function of the survival time $t_{ij}$ given the covariate $\mathbf{x}_{ij}$
$f_0(\cdot)$	baseline density function in the survival models
$g$	parameter in the $g$ -prior for variable selection
$G$	distribution of covariate vectors $\mathbf{x}$ with support on $\mathcal{X} \subseteq \mathbb{R}^p$
$h_{\mathbf{x}_{ij}}(\cdot)$	hazard function of the survival time $t_{ij}$ given the covariate $\mathbf{x}_{ij}$
$h_0(\cdot)$	baseline hazard function in the survival models
$\mathbf{I}_p$	$p \times p$ identity matrix
$I(\cdot)$	the usual indicator function
$J$	number of Bernstein polynomials used for defining $d(\cdot J, \mathbf{w}_J)$
$K$	number of basis functions used for modeling the nonlinear function $u_\ell(\cdot)$
$L(\mathbf{w}_J, \boldsymbol{\theta}, \boldsymbol{\beta}, \mathbf{v})$	likelihood function for $(\mathbf{w}_J, \boldsymbol{\theta}, \boldsymbol{\beta}, \mathbf{v})$
$m$	number of distinct spatial locations
$M$	used to determine the $g$ in the $g$ -prior for variable selection
$n_i$	number of subjects within the $i$ th spatial location, $i = 1, \dots, m$
$n$	total number of subjects in the data, i.e. $n = \sum_{i=1}^m n_i$
$N(a, b^2)$	normal distribution with mean $a$ and variable $b^2$
$N_k(\boldsymbol{\mu}, \boldsymbol{\Sigma})$	$k$ -variate normal distribution with mean $\boldsymbol{\mu}$ and covariance $\boldsymbol{\Sigma}$
$o_{ij}$	number of observations for the time-dependent covariate vector $\mathbf{x}_{ij}(t)$ , $i = 1, \dots, m, j = 1, \dots, n_i$
$p$	dimension of the covariate vector $\mathbf{x}_{ij}$
$p(\cdot)$	generic symbol for prior and posterior density functions
$q$	used to determine the $g$ in the $g$ -prior for variable selection
$r(t_{ij})$	Cox-Snell residual equal to $-\log\{S_{\mathbf{x}_{ij}}(t_{ij})\}$
$\mathbf{R}$	correlation matrix of $\mathbf{v}$ under the GRF prior
$S_{\mathbf{x}_{ij}}(\cdot)$	survival function of the survival time $t_{ij}$ given the covariate $\mathbf{x}_{ij}$
$S_0(\cdot)$	baseline survival function in the survival models
$u_\ell(\cdot)$	nonlinear function for the $\ell$ th covariate, $\ell = 1, \dots, p$
$\mathbf{v} = (v_1, \dots, v_m)'$	vector of frailties
$\mathbf{V}_0$	covariance matrix of the normal $N_2(\boldsymbol{\theta}_0, \mathbf{V}_0)$ prior on $\boldsymbol{\theta}$
$\hat{\mathbf{V}}$	estimate of the covariance of $\hat{\boldsymbol{\theta}}$ under the parametric survival model
$\mathbf{w}_J = (w_1, \dots, w_J)'$	$J$ -vector of positive weights used in the TBP prior
$\mathbf{W}_0$	covariance matrix of the normal $N_p(\boldsymbol{\beta}_0, \mathbf{W}_0)$ prior on $\boldsymbol{\beta}$
$\hat{\mathbf{W}}$	estimate of the covariance of $\hat{\boldsymbol{\beta}}$ under the parametric survival model

Table S1: List of Notations.

Notation	Definition
$\mathbf{x}_{ij}$	$p$ -vector of covariates for subject $ij$ , $i = 1, \dots, m$ , $j = 1, \dots, n_i$
$x_{ij\ell}$	$\ell$ th element of the $\mathbf{x}_{ij}$ , $\ell = 1, \dots, p$
$\mathbf{x}$	generic symbol for $p$ -vector of covariates
$x_\ell$	$\ell$ th element of the $\mathbf{x}$ , $\ell = 1, \dots, p$
$\mathbf{X}$	design matrix associated with $\{\mathbf{x}_{ij}\}$ with mean-centered columns
$\mathbf{X}_\ell$	design matrix associated with $u_\ell(x_\ell)$ with mean-centered columns $\ell = 1, \dots, p$
$z_j$	equals $\log(w_j) - \log(w_J)$
$\mathbf{z}_{J-1}$	equals $(z_1, \dots, z_{J-1})'$

Table S2: List of priors.

Parameter	Prior	Justification
$S_0(\cdot)$	TBP( $\alpha, S_\theta$ )	Selects smooth densities and can be centered at a standard parametric family: one of log-logistic, log-normal, and Weibull.
$\alpha$	$\Gamma(a_\alpha, b_\alpha)$	$\alpha > 0$ acts like the precision in a Dirichlet process controlling how stochastically pliable $S_0$ is close to $S_\theta$ . A gamma prior has been widely used for Dirichlet processes. Defaults: $a_\alpha = b_\alpha = 1$ .
$\beta$	$N_p(\beta_0, \mathbf{W}_0)$	Gaussian is common for regression effects. Defaults: $\beta_0 = \mathbf{0}$ , $\mathbf{W}_0 = 10^{10}\mathbf{I}_p$ or $\mathbf{W}_0 = gn(\mathbf{X}'\mathbf{X})^{-1}$ when the SSVS is performed.
$\theta$	$N_2(\theta_0, \mathbf{V}_0)$	Centering distribution $S_\theta$ is parameterized so that $\theta$ is defined on $\mathbb{R}^2$ , so a Gaussian prior is appropriate. Defaults: $\theta_0 = \hat{\theta}$ , $\mathbf{V}_0 = 10\hat{\mathbf{V}}$ . Note here we assume a somewhat informative prior on $\theta$ to obviate confounding between $\theta$ and $\mathbf{w}_J$ .
$\mathbf{v}$	ICAR( $\tau^2$ )	When clusters are formed by spatial regions and spatial smoothing is of interest, the ICAR prior is commonly used for modeling the frailties in survival models.
$\mathbf{v}$	GRF( $\tau^2, \phi$ )	Very common prior for georeferenced data.
$\mathbf{v}$	IID( $\tau^2$ )	When spatial dependence among clusters is not of interest, the IID Gaussian frailties are commonly assumed.
$\tau^{-2}$	$\Gamma(a_\tau, b_\tau)$	The gamma distribution is a conjugate prior on $\tau^{-2}$ . Defaults: $a_\tau = b_\tau = 0.001$ .
$\phi$	$\Gamma(a_\phi, b_\phi)$	The range parameter $\phi$ is positive and the gamma prior is a natural choice. Defaults: $a_\phi = 2$ and $b_\phi = (a_\phi - 1)/\phi_0$ so that the prior of $\phi$ has mode at $\phi_0$ , where $\phi_0$ satisfies $\rho(\mathbf{s}', \mathbf{s}''; \phi_0) = 0.001$ with $\ \mathbf{s}', \mathbf{s}''\  = \max_{i,j} \ \mathbf{s}_i - \mathbf{s}_j\ $ .
$\gamma$	$\prod_{\ell=1}^p \text{Bern}(q_\ell)$	Commonly used for Bayesian variable selection (e.g. Kuo and Mallick, 1998). Defaults: $q_\ell = 0.5$ , $\ell = 1, \dots, p$ .
$\xi_\ell$	$N_K(\mathbf{0}, \mathbf{S}_\xi)$	Here $\mathbf{S}_\xi = gn(\mathbf{X}'_\ell \mathbf{X}_\ell)^{-1}$ was chosen following the idea of informative $g$ -prior introduced Appendix E.

## Appendix A MCMC Sampling

The joint posterior distribution for all parameters is given by

$$\begin{aligned}
\mathcal{L}(\boldsymbol{\beta}, \boldsymbol{\theta}, \mathbf{w}_J, \alpha, \mathbf{v}, \tau^2, \phi) &\propto L(\mathbf{w}_J, \boldsymbol{\theta}, \boldsymbol{\beta}, \mathbf{v}) \\
&\times \exp \left\{ -\frac{1}{2}(\boldsymbol{\beta} - \boldsymbol{\beta}_0)' \mathbf{W}_0^{-1}(\boldsymbol{\beta} - \boldsymbol{\beta}_0) \right\} \\
&\times \exp \left\{ -\frac{1}{2}(\boldsymbol{\theta} - \boldsymbol{\theta}_0)' \mathbf{V}_0^{-1}(\boldsymbol{\theta} - \boldsymbol{\theta}_0) \right\} \\
&\times \frac{\Gamma(\alpha J)}{\Gamma(\alpha)^J} \prod_{j=1}^J (w_j)^{\alpha-1} \times \alpha^{a\alpha-1} \exp\{-b_\alpha \alpha\} \\
&\times (\tau^{-2})^{\frac{\text{rank}(\mathbf{C})}{2}} \exp \left\{ -\frac{1}{2\tau^2} \mathbf{v}' \mathbf{C} \mathbf{v} \right\} \times (\tau^{-2})^{a\tau-1} \exp\{-b_\tau \tau^{-2}\} \\
&\times p(\phi) |\mathbf{C}|^{1/2}
\end{aligned} \tag{A.1}$$

For the GRF prior,  $\mathbf{C} = \mathbf{R}^{-1}$  and  $p(\phi) = \phi^{a_\phi-1} \exp\{-b_\phi \phi\}$ . The ICAR prior does not need  $p(\phi) |\mathbf{C}|^{1/2}$ , and  $\mathbf{C} = \mathbf{F}_e - \mathbf{E}$ , where  $\mathbf{F}_e$  is an  $m \times m$  diagonal matrix with  $\mathbf{F}_e[i, i] = e_{i+}$ . For the IID prior,  $p(\phi) |\mathbf{C}|^{1/2}$  is also not needed and  $\mathbf{C} = \mathbf{I}_m$  is an identity matrix.

Note that when  $w_j = 1/J$  the underlying parametric model with  $S_0(t) = S_\theta(t)$  is obtained, so a fit from a standard parametric survival model can provide starting values for the TBP survival model. Let  $\hat{\boldsymbol{\theta}}$  and  $\hat{\boldsymbol{\beta}}$  denote the parametric point estimates of  $\boldsymbol{\theta}$  and  $\boldsymbol{\beta}$ , and let  $\hat{\mathbf{V}}$  and  $\hat{\mathbf{W}}$  denote their asymptotic covariance matrices, respectively. These estimates can be easily obtained by running the proposed MCMC below with  $w_j \equiv 1/J$  and relatively vague priors on  $(\boldsymbol{\theta}, \boldsymbol{\beta})$ .

**Step 1:** Update  $\mathbf{w}_J$ .

Set  $\mathbf{z}_{J-1} = (z_1, \dots, z_{J-1})'$  with  $z_j = \log(w_j) - \log(w_J)$ . The full conditional distribution for  $\mathbf{z}_{J-1}$  is

$$p(\mathbf{z}_{J-1} | \text{else}) \propto L(\mathbf{w}_J, \boldsymbol{\theta}, \boldsymbol{\beta}, \mathbf{v}) \times \prod_{j=1}^J \left[ \frac{e^{z_j}}{\sum_{k=1}^J e^{z_k}} \right]^\alpha,$$

where  $z_J = 0$ . The vector  $\mathbf{z}_{J-1}$  can be updated using adaptive Metropolis samplers (Haario et al., 2001). Suppose we are currently in iteration  $l$  and have sampled the states  $\mathbf{z}_{J-1}^{(1)}, \dots, \mathbf{z}_{J-1}^{(l-1)}$ . We select an index  $l_0$  (e.g.,  $l_0 = 5000$ ) for the length of an initial period and define

$$\boldsymbol{\Sigma}_l = \begin{cases} \boldsymbol{\Sigma}_0, & l \leq l_0 \\ \frac{(2.4)^2}{d} (\mathcal{C}_l + 10^{-10} \mathbf{I}_d) & l > l_0. \end{cases}$$

Here  $\mathcal{C}_l$  is the sample variance of  $\mathbf{z}_{J-1}^{(1)}, \dots, \mathbf{z}_{J-1}^{(l-1)}$ ,  $d = J - 1$  is the dimension of  $\mathbf{z}_{J-1}$ , and  $\boldsymbol{\Sigma}_0$  is an initial diagonal covariance matrix of  $\mathbf{z}$ , defined so that the variance of  $z_j$  is 0.16. The choice of 0.16 is based on extensive simulation studies; other choices (as long as it is not too small or large) will have little impact on posterior inferences. We generate  $\mathbf{z}_{J-1}^* = (z_1^*, \dots, z_{J-1}^*)'$  from  $N_{J-1}(\mathbf{z}_{J-1}^{(l-1)}, \boldsymbol{\Sigma}_l)$  and accept it with probability

$$\min \left\{ 1, \frac{p(\mathbf{z}_{J-1}^* | \text{else})}{p(\mathbf{z}_{J-1}^{(l-1)} | \text{else})} \right\}.$$

**Step 2: Update  $\theta$ .**

The full conditional distribution for  $\theta$  is

$$p(\theta|\text{else}) \propto L(\mathbf{w}_J, \theta, \beta, \mathbf{v}) \times \exp \left\{ -\frac{1}{2}(\theta - \theta_0)' \mathbf{V}_0^{-1}(\theta - \theta_0) \right\}.$$

The centering distribution parameters  $\theta$  are updated via adaptive Metropolis samplers. At iteration  $l$ , each candidate is sampled as  $\theta^* \sim N_2(\theta^{(l-1)}, \Sigma_l)$  and accepted with probability

$$\min \left\{ 1, \frac{p(\theta^*|\text{else})}{p(\theta^{(l-1)}|\text{else})} \right\}.$$

where  $\Sigma_l$  is defined similarly as above, but with  $\Sigma_0$  set to be  $\hat{\mathbf{V}}$ .

**Step 3: Update  $\beta$ .**

The full conditional distribution for  $\beta$  is

$$p(\beta|\text{else}) \propto L(\mathbf{w}_J, \theta, \beta, \mathbf{v}) \times \exp \left\{ -\frac{1}{2}(\beta - \beta_0)' \mathbf{W}_0^{-1}(\beta - \beta_0) \right\}.$$

The survival model coefficients  $\beta$  are updated via adaptive Metropolis samplers as well with proposal  $\beta^* \sim N_p(\beta^{(l-1)}, \Sigma_l)$  and acceptance probability

$$\min \left\{ 1, \frac{p(\beta^*|\text{else})}{p(\beta^{(l-1)}|\text{else})} \right\}.$$

where  $\Sigma_l$  is defined similarly as above with  $\Sigma_0 = \hat{\mathbf{W}}$ .

**Step 4: Update  $\alpha$ .**

The full conditional distribution for  $\alpha$  is

$$p(\alpha|\text{else}) \propto \frac{\Gamma(\alpha J)}{\Gamma(\alpha)^J} \prod_{j=1}^J (w_j)^{\alpha-1} \times \alpha^{a\alpha-1} \exp\{-b_\alpha \alpha\}.$$

The precision parameter  $\alpha$  is updated via adaptive Metropolis samplers with normal proposal  $\alpha^* \sim N_1(\alpha^{(l-1)}, \Sigma_l)$  with  $\Sigma_l$  is defined similarly as above with  $\Sigma_0 = 0.16$ , and the acceptance probability is

$$\min \left\{ 1, \frac{p(\alpha^*|\text{else})}{p(\alpha^{(l-1)}|\text{else})} \right\}.$$

**Step 5: Update  $\mathbf{v}$ .**

Let  $L(\mathbf{w}_J, \theta, \beta, \mathbf{v}) = \prod_{i=1}^m \prod_{j=1}^{n_i} L_{ij}(\mathbf{w}_J, \theta, \beta, \mathbf{v})$ . For the ICAR prior, the full conditional distribution for  $v_i$ ,  $i = 1, \dots, m$ , is

$$p(v_i|\text{else}) \propto \prod_{j=1}^{n_i} L_{ij}(\mathbf{w}_J, \theta, \beta, \mathbf{v}) \exp \left\{ -\frac{e_{i+}}{2\tau^2} \left( v_i - \sum_{j=1}^m e_{ij} v_j / e_{i+} \right)^2 \right\}.$$

The  $v_j$  is updated via Metropolis-Hastings sampling steps with proposal  $v_j^* \sim N(v_j^{(l-1)}, \tau^2/e_{j+})$ . The candidate  $v_j^*$  is accepted with probability

$$\min \left\{ 1, \frac{p(v_j^*|\text{else})}{p(v_j^{(l-1)}|\text{else})} \right\}.$$

After each individual frailty update, the vector of  $\mathbf{v}$  is updated to have sample mean zero through  $\mathbf{v} \leftarrow \mathbf{v} - \frac{1}{m} \mathbf{1}'_m \mathbf{v}$ . Although *ad hoc*, this approach to enforcing the sum-to-zero constraint on  $v_1, \dots, v_m$  has negligible effect on the posterior and has been advocated by many authors, e.g. Banerjee et al. (2014) and Lang and Brezger (2004).

For the IID prior, the full conditional distribution for  $v_i$ ,  $i = 1, \dots, m$ , is

$$p(v_i|\text{else}) \propto \prod_{j=1}^{n_i} L_{ij}(\mathbf{w}_J, \boldsymbol{\theta}, \boldsymbol{\beta}, \mathbf{v}) \exp \left\{ -\frac{1}{2\tau^2} v_i^2 \right\}.$$

The  $v_j$  is updated via Metropolis-Hastings sampling steps with proposal  $v_j^* \sim N(v_j^{(l-1)}, \tau^2)$ . The candidate  $v_j^*$  is accepted with probability

$$\min \left\{ 1, \frac{p(v_j^*|\text{else})}{p(v_j^{(l-1)}|\text{else})} \right\}.$$

For the GRF prior, the full conditional distribution for  $v_i$ ,  $i = 1, \dots, m$ , is

$$p(v_i|\text{else}) \propto \prod_{j=1}^{n_i} L_{ij}(\mathbf{w}_J, \boldsymbol{\theta}, \boldsymbol{\beta}, \mathbf{v}) \exp \left\{ -\frac{p_{ii}}{2\tau^2} \left( v_i + \sum_{\{j:j \neq i\}} p_{ij} v_j / p_{ii} \right)^2 \right\},$$

where  $p_{ij}$  is the  $(i, j)$  element of  $\mathbf{R}^{-1}$ . The  $v_j$  is updated via Metropolis-Hastings sampling steps with proposal  $v_j^* \sim N(v_j^{(l-1)}, \tau^2/p_{ii})$ . The candidate  $v_j^*$  is accepted with probability

$$\min \left\{ 1, \frac{p(v_j^*|\text{else})}{p(v_j^{(l-1)}|\text{else})} \right\}.$$

**Step 6:** Update  $\tau^2$ .

The full conditional distribution for  $\tau^{-2}$  is

$$p(\tau^{-2}|\text{else}) \propto (\tau^{-2})^{a_\tau + \frac{\text{rank}(\mathbf{C})}{2} - 1} \exp \left\{ -\left[ b_\tau + \frac{1}{2} \mathbf{v}' \mathbf{C} \mathbf{v} \right] \tau^{-2} \right\}.$$

Thus  $\tau^{-2}$  is sampled from  $\Gamma(a_\tau^*, b_\tau^*)$ , where  $a_\tau^* = a_\tau + \frac{\text{rank}(\mathbf{C})}{2} - 1$  and  $b_\tau^* = b_\tau + \frac{1}{2} \mathbf{v}' \mathbf{C} \mathbf{v}$ .

**Step 7:** Update  $\phi$  for georeferenced data.

The full conditional distribution for  $\phi$  is

$$p(\phi|\text{else}) \propto |\mathbf{R}|^{-1/2} \exp \left\{ -\frac{1}{2\tau^2} \mathbf{v}' \mathbf{R}^{-1} \mathbf{v} \right\} \phi^{a_\tau - 1} \exp \{-b_\tau \phi\}$$

The range parameter  $\phi$  is updated via adaptive Metropolis samplers with normal proposal  $\phi^* \sim N_1(\phi^{(l-1)}, \boldsymbol{\Sigma}_l)$  with  $\boldsymbol{\Sigma}_l$  is defined similarly as above with  $\boldsymbol{\Sigma}_0 = 0.16$ , and the acceptance probability is

$$\min \left\{ 1, \frac{p(\phi^*|\text{else})}{p(\phi^{(l-1)}|\text{else})} \right\}.$$

**Step 8:** Update  $\boldsymbol{\gamma}$  when variable selection is performed.

When variable selection is performed, all  $\boldsymbol{\beta}$ s in steps 1-7 need to be replaced by  $\boldsymbol{\gamma} \odot \boldsymbol{\beta}$ , where  $\odot$

denotes componentwise multiplication. Then each  $\gamma_j$  is generated from its full conditional, i.e. a Bernoulli distribution with the success probability

$$\frac{q_j}{q_j + (1 - q_j)L(\mathbf{w}_J, \boldsymbol{\theta}, \boldsymbol{\gamma}_{j0} \odot \boldsymbol{\beta}, \mathbf{v})/L(\mathbf{w}_J, \boldsymbol{\theta}, \boldsymbol{\gamma}_{j1} \odot \boldsymbol{\beta}, \mathbf{v})},$$

where the vector  $\boldsymbol{\gamma}_{j0}$  ( $\boldsymbol{\gamma}_{j1}$ ) is obtained from  $\boldsymbol{\gamma}$  with the  $j$ th element replaced by 0 (1).

## Appendix B The Full Scale Approximation

For georeferenced data, a computational bottleneck of the MCMC sampling scheme is inverting the  $m \times m$  matrix  $\mathbf{R}$ , which typically has computational cost  $O(m^3)$ . In this section, we introduce a full scale approximation (FSA) approach proposed by Sang and Huang (2012), which provides a high quality approximation to the correlation function  $\rho$  at both the large and the small spatial scales, such that the inverse of  $\mathbf{R}$  can be substantially sped up for large value of  $m$ , e.g.,  $m \geq 500$ .

Consider a fixed set of ‘‘knots’’  $\mathcal{S}^* = \{\mathbf{s}_1^*, \dots, \mathbf{s}_A^*\}$  chosen from the study region. These knots can be chosen using the function `cover.design` within the R package `fields`, which computes space-filling coverage designs using the swapping algorithm (Johnson et al., 1990). Let  $\rho(\mathbf{s}, \mathbf{s}')$  be the correlation between locations  $\mathbf{s}$  and  $\mathbf{s}'$ . The FSA approach approximates the correlation function  $\rho(\mathbf{s}, \mathbf{s}')$  with

$$\rho^\dagger(\mathbf{s}, \mathbf{s}') = \rho_l(\mathbf{s}, \mathbf{s}') + \rho_s(\mathbf{s}, \mathbf{s}'). \quad (\text{B.2})$$

The  $\rho_l(\mathbf{s}, \mathbf{s}')$  in (B.2) is the reduced-rank part capturing the long-scale spatial dependence, defined as  $\rho_l(\mathbf{s}, \mathbf{s}') = \boldsymbol{\rho}'(\mathbf{s}, \mathcal{S}^*)\boldsymbol{\rho}_{AA}^{-1}(\mathcal{S}^*, \mathcal{S}^*)\boldsymbol{\rho}(\mathbf{s}', \mathcal{S}^*)$ , where  $\boldsymbol{\rho}(\mathbf{s}, \mathcal{S}^*) = [\rho(\mathbf{s}, \mathbf{s}_i^*)]_{i=1}^A$  is an  $A \times 1$  vector, and  $\boldsymbol{\rho}_{AA}(\mathcal{S}^*, \mathcal{S}^*) = [\rho(\mathbf{s}_i^*, \mathbf{s}_j^*)]_{i,j=1}^A$  is an  $A \times A$  correlation matrix at knots  $\mathcal{S}^*$ . However,  $\rho_l(\mathbf{s}, \mathbf{s}')$  cannot well capture the short-scale dependence due to the fact that it discards entirely the residual part  $\rho(\mathbf{s}, \mathbf{s}') - \rho_l(\mathbf{s}, \mathbf{s}')$ . The idea of FSA is to add a small-scale part  $\rho_s(\mathbf{s}, \mathbf{s}')$  as a sparse approximate of the residual part, defined by  $\rho_s(\mathbf{s}, \mathbf{s}') = \{\rho(\mathbf{s}, \mathbf{s}') - \rho_l(\mathbf{s}, \mathbf{s}')\} \Delta(\mathbf{s}, \mathbf{s}')$ , where  $\Delta(\mathbf{s}, \mathbf{s}')$  is a modulating function, which is specified so that the  $\rho_s(\mathbf{s}, \mathbf{s}')$  can well capture the local residual spatial dependence while still permits efficient computations. Motivated by Konomi et al. (2014), we first partition the total input space into  $B$  disjoint blocks, and then specify  $\Delta(\mathbf{s}, \mathbf{s}')$  in a way such that the residuals are independent across input blocks, but the original residual dependence structure within each block is retained. Specifically, the function  $\Delta(\mathbf{s}, \mathbf{s}')$  is taken to be 1 if  $\mathbf{s}$  and  $\mathbf{s}'$  belong to the same block and 0 otherwise. The approximated correlation function  $\rho^\dagger(\mathbf{s}, \mathbf{s}')$  in (B.2) provides an exact recovery of the true correlation within each block, and the approximation errors are  $\rho(\mathbf{s}, \mathbf{s}') - \rho_l(\mathbf{s}, \mathbf{s}')$  for locations  $\mathbf{s}$  and  $\mathbf{s}'$  in different blocks. Those errors are expected to be small for most entries because most of these location pairs are farther apart. To determine the blocks, we first use the R function `cover.design` to choose  $B \leq m$  locations among the  $m$  locations forming  $B$  blocks, then assign each  $\mathbf{s}_i$  to the block that is closest to  $\mathbf{s}_i$ . Here  $B$  does not need to be equal to  $A$ . When  $B = 1$ , no approximation is applied to the correlation  $\rho$ . When  $B = m$ , it reduces to the approach of Finley et al. (2009), so the local residual spatial dependence may not be well captured.

Applying the above FSA approach to approximate the correlation function  $\rho(\mathbf{s}, \mathbf{s}')$ , we can approximate the correlation matrix  $\mathbf{R}$  with

$$\boldsymbol{\rho}_{mm}^\dagger = \boldsymbol{\rho}_l + \boldsymbol{\rho}_s = \boldsymbol{\rho}_{mA}\boldsymbol{\rho}_{AA}^{-1}\boldsymbol{\rho}'_{mA} + (\boldsymbol{\rho}_{mm} - \boldsymbol{\rho}_{mA}\boldsymbol{\rho}_{AA}^{-1}\boldsymbol{\rho}'_{mA}) \circ \boldsymbol{\Delta}, \quad (\text{B.3})$$

where  $\boldsymbol{\rho}_{mA} = [\rho(\mathbf{s}_i, \mathbf{s}_j^*)]_{i=1:m, j=1:A}$ ,  $\boldsymbol{\rho}_{AA} = [\rho(\mathbf{s}_i^*, \mathbf{s}_j^*)]_{i,j=1}^A$ , and  $\boldsymbol{\Delta} = [\Delta(\mathbf{s}_i, \mathbf{s}_j)]_{i,j=1}^m$ . Here, the notation ‘‘ $\circ$ ’’ represents the element-wise matrix multiplication. To avoid numerical instability, we



add a small nugget effect  $\epsilon = 10^{-10}$  when define  $\mathbf{R}$ , that is,  $\mathbf{R} = (1 - \epsilon)\boldsymbol{\rho}_{mm} + \epsilon\mathbf{I}_m$ . It follows from equation (B.3) that  $\mathbf{R}$  can be approximated by

$$\mathbf{R}^\dagger = (1 - \epsilon)\boldsymbol{\rho}_{mm}^\dagger + \epsilon\mathbf{I}_m = (1 - \epsilon)\boldsymbol{\rho}_{mA}\boldsymbol{\rho}_{AA}^{-1}\boldsymbol{\rho}'_{mA} + \mathbf{R}_s,$$

where  $\mathbf{R}_s = (1 - \epsilon)(\boldsymbol{\rho}_{mm} - \boldsymbol{\rho}_{mA}\boldsymbol{\rho}_{AA}^{-1}\boldsymbol{\rho}'_{mA}) \circ \boldsymbol{\Delta} + \epsilon\mathbf{I}_m$ . Applying the Sherman-Woodbury-Morrison formula for inverse matrices, we can approximate  $\mathbf{R}^{-1}$  by

$$\left(\mathbf{R}^\dagger\right)^{-1} = \mathbf{R}_s^{-1} - (1 - \epsilon)\mathbf{R}_s^{-1}\boldsymbol{\rho}_{mA} \left[\boldsymbol{\rho}_{AA} + (1 - \epsilon)\boldsymbol{\rho}'_{mA}\mathbf{R}_s^{-1}\boldsymbol{\rho}_{mA}\right]^{-1} \boldsymbol{\rho}'_{mA}\mathbf{R}_s^{-1}. \quad (\text{B.4})$$

In addition, the determinant of  $\mathbf{R}$  can be approximated by

$$\det\left(\mathbf{R}^\dagger\right) = \det\left\{\boldsymbol{\rho}_{AA} + (1 - \epsilon)\boldsymbol{\rho}'_{mA}\mathbf{R}_s^{-1}\boldsymbol{\rho}_{mA}\right\} \det(\boldsymbol{\rho}_{AA})^{-1} \det(\mathbf{R}_s). \quad (\text{B.5})$$

Since the  $m \times m$  matrix  $\mathbf{R}_s$  is a block matrix, the right-hand sides of equations (B.4) and (B.5) involve only inverses and determinants of  $A \times A$  low-rank matrices and  $m \times m$  block diagonal matrices. Thus the computational complexity can be greatly reduced relative to the expensive computational cost of using original correlation function for large value of  $m$ .

## Appendix C The DIC and LPML Criteria

To set notation, denote by  $\mathcal{D}$  the observed dataset, by  $\mathcal{D}_i$  the  $i$ th data point, and by  $\mathcal{D}_{-i}$  the dataset with  $\mathcal{D}_i$  removed,  $i = 1, \dots, n$ . Let  $\Omega$  denote the entire collection of model parameters under a particular model,  $L(\mathcal{D}|\Omega)$  be the likelihood function based on observed data  $\mathcal{D}$ , and  $L_i(\cdot|\Omega)$  be the likelihood contribution based on  $\mathcal{D}_i$ . Suppose  $\{\Omega^{(1)}, \dots, \Omega^{(\mathcal{L})}\}$  are random draws from the full posterior  $p_{post}(\Omega|\mathcal{D})$ . Let  $\hat{\Omega} = \sum_{l=1}^{\mathcal{L}} \Omega^{(l)} / \mathcal{L}$  be the posterior mean estimate for  $\Omega$ .

The DIC, a generalization of the Akaike information criterion (AIC), is commonly used for comparing complex hierarchical models for which the asymptotic justification of AIC is not appropriate. The DIC is defined as

$$\text{DIC} = -2 \log L(\mathcal{D}|\hat{\Omega}) + 2p_D, \quad (\text{C.6})$$

where

$$p_D = 2 \left( \log L(\mathcal{D}|\hat{\Omega}) - \frac{1}{\mathcal{L}} \sum_{l=1}^{\mathcal{L}} \log L(\mathcal{D}|\Omega^{(l)}) \right)$$

is referred to as the effective number of parameters measuring the model complexity. Similar to AIC, a smaller value of DIC indicates a better fit model.

The definition of LPML is based on the conditional predictive ordinate (CPO) statistic. The CPO for data point  $\mathcal{D}_i$  is given by

$$\text{CPO}_i = f(\mathcal{D}_i|\mathcal{D}_{-i}) = \int L_i(\mathcal{D}_i|\Omega) p_{post}(\Omega|\mathcal{D}_{-i}) d\Omega,$$

where  $p_{post}(\cdot|\mathcal{D}_{-i})$  is the posterior density of  $\Omega$  give  $\mathcal{D}_{-i}$ . Let  $\text{CPO}_{i,1}$  and  $\text{CPO}_{i,2}$  denote the CPO for the  $i$ th data point under models 1 and 2, respectively. The ratio  $\text{CPO}_{i,1}/\text{CPO}_{i,2}$  measures how well model 1 supports the data point  $\mathcal{D}_i$  relative to model 2, based on the remaining data  $\mathcal{D}_{-i}$ . The product of the CPO ratios gives an overall aggregate summary of how well supported the data are by model 1 relative to model 2 and is called the pseudo Bayes factor (PBF),

$$B_{12} = \prod_{i=1}^n \frac{\text{CPO}_{i,1}}{\text{CPO}_{i,2}}.$$

It is well known that Bayes factors (Kass and Raftery, 1995; Han and Carlin, 2001) are usually difficult to obtain in practice. The PBF is a surrogate for the more traditional Bayes factor and can be interpreted similarly, but is more analytically tractable, much less sensitive to prior assumptions, and does not suffer from Lindley’s paradox.

As noted by Gelfand and Dey (1994), one can use importance sampling to estimate  $\text{CPO}_i$  by

$$\left\{ \frac{1}{\mathcal{L}} \sum_{l=1}^{\mathcal{L}} \frac{1}{L_i(\mathcal{D}_i|\Omega^{(l)})} \right\}^{-1}.$$

However, these estimates may be unstable since the weights  $\omega_{i,l} = 1/L_i(\mathcal{D}_i|\Omega^{(l)})$  can have infinite variance (Epifani et al., 2008), depending on the tail behavior of  $p_{post}(\Omega|\mathcal{D}_{-i})$  relative to  $L_i(\mathcal{D}_i|\Omega)$  as a function of  $\Omega$ . To stabilize the weights, Vehtari and Gelman (2014) suggest replacing  $\omega_{i,l}$  with  $\tilde{\omega}_{i,l} = \min\{\omega_{i,l}, \sqrt{\mathcal{L}\bar{\omega}_i}\}$ , where  $\bar{\omega}_i = \sum_{l=1}^{\mathcal{L}} \omega_{i,l}/\mathcal{L}$ . Therefore, the stabilized estimate of the CPO statistic is

$$\widehat{\text{CPO}}_i = \frac{\sum_{l=1}^{\mathcal{L}} L_i(\mathcal{D}_i|\Omega^{(l)})\tilde{\omega}_{i,l}}{\sum_{l=1}^{\mathcal{L}} \tilde{\omega}_{i,l}}.$$

Finally, the LPML is defined as

$$\text{LPML} = \sum_{i=1}^n \log \widehat{\text{CPO}}_i. \quad (\text{C.7})$$

A further improved estimate was recently proposed by Vehtari et al. (2017) using Pareto-smoothed importance sampling; this version will be implemented in later versions of the R package.

The LPML can be viewed as a predictive measure that generalizes leave-one-out cross-validated prediction error to more heavily penalize “bad predictions.” Consider the frequentist LPML proposed by Geisser and Eddy (1979) for normal-errors regression data. Let  $y_i \stackrel{\text{ind.}}{\sim} N(\mathbf{x}'_i\boldsymbol{\beta}, \sigma^2)$ ; then

$$\text{CPO}_i = \frac{1}{\sqrt{2\pi}\hat{\sigma}_i} \exp \left\{ -\frac{(y_i - \mathbf{x}'_i\hat{\boldsymbol{\beta}}_i)^2}{2\hat{\sigma}_i^2} \right\},$$

where  $(\hat{\boldsymbol{\beta}}_i, \hat{\sigma}_i)$  is the MLE of  $(\boldsymbol{\beta}, \sigma)$  leaving out  $(\mathbf{x}_i, y_i)$ . Then

$$-\text{LPML} = \underbrace{\sum_{i=1}^n \frac{1}{2\hat{\sigma}_i} (y_i - \hat{y}_{-i})^2}_{\text{squared bias}} + \underbrace{\sum_{i=1}^n \log \hat{\sigma}_i}_{\text{variance}} + \text{constant}.$$

This generalizes to any location-scale family, e.g. parametric survival models  $\log t_i = \mathbf{x}'_i\boldsymbol{\beta} + \epsilon_i$ , where  $\epsilon_i$  has a scaled standard extreme value distribution, scaled log-logistic distribution, or scaled normal distribution yielding common Weibull, log-logistic, and log-normal regression models. Note that unlike the usual predicted residual error sum of squares (PRESS) statistic the bias terms are weighted by the variability of the prediction: “bad” predictions with less variability (more precision) provide much more discrepancy than “bad” predictions with large variability. Having both bias and variance pieces, the LPML is of similar form to the L-measure (Ibrahim et al., 2001), but more naturally generalizes to survival data; note that Ibrahim et al. (2001) advocating taking the log of the survival time and require a different L-measure for each family of distributions.

A Bayesian might view the frequentist  $\text{CPO}_i$  using the MLE above as overoptimistic. The MLE is the posterior mode under a flat prior and sampling variability is not taken into account. Instead, one might want to average the  $\text{CPO}_i$  statistic over the (perhaps asymptotic) estimated

sampling distribution of  $\Omega_i$ , e.g.  $\Omega_i \overset{\bullet}{\sim} N(\hat{\Omega}_i, \mathbf{V}_i)$ . Equivalently, and more precisely, the Bayesian approach averages the predictive density for a new observation with covariates  $\mathbf{x}_i$  over the leave- $i$ -out posterior  $[\Omega|\mathcal{D}_{-i}]$ . Thus the Bayesian LPML used here can be viewed as a measure similar to PRESS or prediction error, but a properly pessimistic one that averages over the (non-asymptotic) sampling distribution of the parameters. The more sampling variability there is (reflecting smaller sampler sizes  $n$ ), the more heavily each CPO $_i$  is penalized.

In addition to DIC and LPML, the Watanabe-Akaike information criterion (WAIC) (Watanabe, 2010) has also gained popularity in recent years due to its stability compared to DIC (Gelman et al., 2014; Vehtari and Gelman, 2014). The WAIC is defined as

$$\text{WAIC} = -2 \sum_{i=1}^n \log \left( \frac{1}{\mathcal{L}} \sum_{l=1}^{\mathcal{L}} L_i(\mathcal{D}_i|\Omega^{(l)}) \right) + 2p_W, \quad (\text{C.8})$$

where

$$p_W = \sum_{i=1}^n \left[ \frac{1}{\mathcal{L}-1} \sum_{l=1}^{\mathcal{L}} \left\{ \log L_i(\mathcal{D}_i|\Omega^{(l)}) - \frac{1}{\mathcal{L}} \sum_{k=1}^{\mathcal{L}} \log L_i(\mathcal{D}_i|\Omega^{(k)}) \right\}^2 \right]$$

is the effective number of parameters. A smaller value of WAIC indicates a better predictive model. WAIC can be viewed as an approximation to  $-2 \sum_{i=1}^n \log \text{CPO}_i$  (Gelman et al., 2014), so WAIC is also used to compare models' predictive performance. The WAIC has been implemented in the function `survregbayes` and saved in its returned object.

## Appendix D Parametric vs. Nonparametric $S_0(\cdot)$

Many authors have found parametric models to fit as well or better than competing semiparametric models (Cox and Oakes, 1984, p. 123; Nardi and Schemper, 2003). Here, testing for the adequacy of the simpler underlying parametric model is developed. The proposed semiparametric models have their baseline survival functions centered at a parametric family  $S_\theta(t)$ . Note that  $\mathbf{z}_{J-1} = \mathbf{0}$  implies  $S_0(t) = S_\theta(t)$ . Therefore, testing  $H_0 : \mathbf{z}_{J-1} = \mathbf{0}$  versus  $H_1 : \mathbf{z}_{J-1} \neq \mathbf{0}$  leads to the comparison of the semiparametric model with the underlying parametric model. Let  $BF_{10}$  be the Bayes factor between  $H_1$  and  $H_0$ . Zhou et al. (2017) proposed to estimate  $BF_{10}$  by a large-sample approximation to the generalized Savage-Dickey density ratio (Verdinelli and Wasserman, 1995). Adapting their approach  $BF_{10}$  is estimated

$$\widehat{BF}_{10} = \frac{p(\mathbf{0}|\hat{\alpha})}{N_{J-1}(\mathbf{0}; \hat{\mathbf{m}}, \hat{\Sigma})}, \quad (\text{D.9})$$

where  $p(\mathbf{0}|\alpha) = \Gamma(\alpha J)/[J^\alpha \Gamma(\alpha)]^J$  is the prior density of  $\mathbf{z}_{J-1}$  evaluated at  $\mathbf{z}_{J-1} = \mathbf{0}$ ,  $\hat{\alpha}$  is the posterior mean of  $\alpha$ ,  $N_p(\cdot; \mathbf{m}, \Sigma)$  denotes a  $p$ -variable normal density with mean  $\mathbf{m}$  and covariance  $\Sigma$ , and  $\hat{\mathbf{m}}$  and  $\hat{\Sigma}$  are posterior mean and covariance of  $\mathbf{z}_{J-1}$ .

## Appendix E Variable Selection

There is a large amount of literature on Bayesian variable selection methods; see O'Hara and Sillanpää (2009) for a comprehensive review. Let  $\mathbf{x} = (x_1, \dots, x_p)'$  denote the  $p$ -vector of covariates in general. The most direct approach is to multiply  $\beta_\ell$  by a latent Bernoulli variable  $\gamma_\ell$  for  $\ell = 1, \dots, p$ , where  $\gamma_\ell = 1$  indicates the presence of  $x_\ell$  in the model, and then assume an appropriate prior on  $(\boldsymbol{\beta}, \boldsymbol{\gamma})$ , where  $\boldsymbol{\gamma} = (\gamma_1, \dots, \gamma_p)'$ . Kuo and Mallick (1998) considered an independent prior

$p(\boldsymbol{\beta}, \boldsymbol{\gamma}) = N_p(\mathbf{0}, \mathbf{W}_0) \times \prod_{\ell=1}^p \text{Bern}(q_\ell)$ , where  $\mathbf{W}_0$  was taken as a diagonal matrix yielding a diffuse prior on  $\boldsymbol{\beta}$ , and  $q_\ell$  is a prior probability of including  $x_\ell$  in the model. The resulting MCMC algorithm does not require any tuning, but mixing can be poor if the prior on  $\boldsymbol{\beta}$  is too diffuse (O’Hara and Sillanpää, 2009). The  $g$ -prior of Zellner (1983) and its various extensions (Bové et al., 2011; Hanson et al., 2014) have been widely used for variable selection. We consider one such prior adapted for use in the semiparametric survival models considered here. Specifically, the same prior as Kuo and Mallick (1998) is considered, but with

$$\boldsymbol{\beta} \sim N_p(\mathbf{0}, gn(\mathbf{X}'\mathbf{X})^{-1}), \quad (\text{E.10})$$

where  $\mathbf{X}$  is the usual design matrix, but with mean-centered covariates, i.e.  $\mathbf{1}'_n \mathbf{X} = \mathbf{0}'_p$ . Assume that the covariate vectors  $\mathbf{x}_{ij}$  arise from a distribution  $G$  with support on  $\mathcal{X} \subseteq \mathbb{R}^p$ , and are independent of  $\boldsymbol{\beta}$ . Following Hanson et al. (2014)  $g$  is set equal to a constant based on prior information on  $e^{\mathbf{x}'\boldsymbol{\beta}}$ , i.e. the relative risks (PH), acceleration factors (AFT), or odds factors (PO) of random subjects  $\mathbf{x}$  relative to their mean  $\int_{\mathcal{X}} \mathbf{x}G(d\mathbf{x})$ . Under the prior (E.10), Hanson et al. (2014) showed that  $\mathbf{x}'\boldsymbol{\beta}$  has an approximately normal distribution with mean 0 and variance  $ng$ . Thus, a simple method of choosing  $g$  is to pick a number  $M$  such that a random  $e^{\mathbf{x}'\boldsymbol{\beta}}$  is less than  $M$  with probability  $q$ . It follows that  $g = [\log M / \Phi^{-1}(q)]^2 / p$ . Here,  $M = 10$  and  $q = 0.9$  are fixed. The MCMC procedure is described in supplementary Appendix A. Posterior output includes a list of sub-models with their posterior probabilities, i.e. a ranking of models much like the best subsets  $C_p$  statistic.

This variable selection method was originally termed “stochastic search variable selection” (SSVS) by George and McCulloch (1993) who instead of using Bernoulli point masses for each regression effect used highly concentrated normal distributions centered at zero. This approach has also been called “spike and slab” variable selection by many authors. A recent review and extensive simulation study by Pavlou et al. (2016) suggests that SVSS can routinely outperform other variable selection approaches. They found that SSVS performed overall the best across many realistic data scenarios for variable selection among methods that also include versions of the LASSO (regular, adaptive, and Bayesian), SCAD, and the elastic net. All methods grossly outperformed backwards elimination; see Table 4 in Pavlou et al. (2016).

## Appendix F Left-Truncation and Time-Dependent Covariates

To avoid an explosion of subscripts, drop the  $ij$  from  $t_{ij}$ , etc. The survival time  $t$  is left-truncated at  $u \geq 0$  if  $u$  is the time when the subject under consideration is first observed. Left-truncation often occurs when age is used as the time scale. Given the observed left-truncated data  $\{(u, a, b, \mathbf{x}, \mathbf{s})\}$ , where  $a \geq u$ , the likelihood contribution is

$$L = [S_{\mathbf{x}}(a) - S_{\mathbf{x}}(b)]^{I\{a < b\}} f_{\mathbf{x}}(a)^{I\{a=b\}} / S_{\mathbf{x}}(u).$$

Note that the left censored data under left-truncation are of the form  $(u, b)$ .

We next discuss how to extend the semiparametric AFT, PH and PO models to handle time-dependent covariates. Let  $\{(u, a, b, \mathbf{x}(t), \mathbf{s}) : u \leq t \leq a\}$  be the observed data with time-dependent covariates and possible left-truncation. Suppose we observe  $\mathbf{x}(t)$  at  $o$  ordered times  $t = t_1, \dots, t_o$ , denoted as  $\mathbf{x}_1, \dots, \mathbf{x}_o$ , respectively, where  $t_1 = u$  and  $t_o \leq a$ . Following Kneib (2006) and Hanson et al. (2009), we assume that  $\mathbf{x}(t)$  is a step function given by

$$\mathbf{x}(t) = \sum_{k=1}^o \mathbf{x}_k I(t_k \leq t < t_{k+1}),$$

where  $t_{o+1} = \infty$ . Assuming the AFT, PH or PO holds conditionally on each interval, the survival function at time  $a$  is

$$\begin{aligned} P(t > a) &= P(t > a | t > t_o) \prod_{k=1}^{o-1} P(t > t_{k+1} | t > t_k) \\ &= \frac{S_{\mathbf{x}_o}(a)}{S_{\mathbf{x}_o}(t_o)} \prod_{k=1}^{o-1} \frac{S_{\mathbf{x}_k}(t_{k+1})}{S_{\mathbf{x}_k}(t_k)}. \end{aligned}$$

This leads to the usual PH model for time-dependent covariates (Cox, 1972), the AFT model first proposed by Prentice and Kalbfleisch (1979), and a particular piecewise PO model.

Returning to the use of subscripts for the  $ij$ th subject, for time-dependent covariates replace  $(u_{ij}, a_{ij}, b_{ij}, \mathbf{x}_{ij}(t), \mathbf{s}_i)$  by a set of new  $o_{ij}$  observations  $(t_{ij,1}, t_{ij,2}, \infty, \mathbf{x}_{ij,1}, \mathbf{s}_i)$ ,  $(t_{ij,2}, t_{ij,3}, \infty, \mathbf{x}_{ij,2}, \mathbf{s}_i)$ ,  $\dots$ ,  $(t_{ij,o_{ij}}, a_{ij}, b_{ij}, \mathbf{x}_{ij,o_{ij}}, \mathbf{s}_i)$  yielding an augmented left-truncated data set of size  $\sum_{i=1}^m \sum_{j=1}^{n_i} o_{ij}$ . Then the likelihood function becomes

$$\begin{aligned} L(\mathbf{w}_J, \boldsymbol{\theta}, \boldsymbol{\beta}, \mathbf{v}) &= \prod_{i=1}^m \prod_{j=1}^{n_i} \left\{ \left[ S_{\mathbf{x}_{ij,o_{ij}}}(a_{ij}) - S_{\mathbf{x}_{ij,o_{ij}}}(b_{ij}) \right]^{I\{a_{ij} < b_{ij}\}} f_{\mathbf{x}_{ij,o_{ij}}}(a_{ij})^{I\{a_{ij} = b_{ij}\}} / S_{\mathbf{x}_{ij,o_{ij}}}(t_{ij,o_{ij}}) \right. \\ &\quad \left. \times \prod_{k=1}^{o_{ij}-1} \frac{S_{\mathbf{x}_{ij,k}}(t_{ij,k+1})}{S_{\mathbf{x}_{ij,k}}(t_{ij,k})} \right\}. \end{aligned}$$

Note that the derivations above still hold for time-dependent covariates without left-truncation (i.e.  $u_{ij} = 0$  for all  $i$  and  $j$ ).

## Appendix G Partially linear predictors

An additive PH model was first considered by Gray (1992) as

$$h_{\mathbf{x}_{ij}}(t) = h_0(t) \exp\left\{ \mathbf{x}'_{ij} \boldsymbol{\beta} + \sum_{\ell=1}^p u_{\ell}(x_{ij\ell}) \right\},$$

where the nonlinear functions  $u_1(\cdot), \dots, u_p(\cdot)$  are modeled via penalized B-splines with the linear portion removed. Setting some of the  $u_{\ell}(\cdot) \equiv 0$  gives the so-called ‘‘partially linear PH model’’ that has been given a great deal of attention in recent literature. This model has been extended to spatial versions by Kneib (2006) and Hennerfeind et al. (2006) for PH and can be easily fit in R2BayesX.

Additive partially linear predictors can be implemented in the proposed AFT, PH and PO models by simply adding a linear basis expansion for any continuous covariate; cubic B-splines are considered here and illustrated in Section 3.3. Specifically,  $u_{\ell}(\cdot)$  is parameterized as

$$u_{\ell}(\cdot) = \sum_{k=1}^K \xi_{\ell k} B_{\ell k}(\cdot),$$

where  $\{B_{\ell k}(\cdot) : k = 0, \dots, K+1\}$  are the standard cubic B-spline basis functions with knots determined by the data; the first and last basis functions have been dropped to ensure a full-rank model (the linear term is already included). Independent normal priors are considered for  $\boldsymbol{\beta}$  and  $\boldsymbol{\xi}_{\ell} = (\xi_{\ell 1}, \dots, \xi_{\ell K})'$ :

$$\boldsymbol{\beta} \sim N_p(\mathbf{0}, \mathbf{W}_0), \quad \boldsymbol{\xi}_{\ell} \sim N_K(\mathbf{0}, gn(\mathbf{X}'_{\ell} \mathbf{X}_{\ell})^{-1}), \ell = 1, \dots, p$$

where  $\mathbf{W}_0 = 10^{10}\mathbf{I}_p$ ,  $\mathbf{X}_\ell$  is the design matrix for the  $u_\ell(\cdot)$  term, and  $g = [\log 10/\Phi^{-1}(0.9)]^2/K$ . This approach can be viewed as a simplified version of the Bayesian P-splines (Lang and Brezger, 2004) with fewer basis functions and a g-prior “penalty” instead of a random-walk penalty. Note that posterior updating could be inefficient if a large number of basis functions is considered, as  $(\boldsymbol{\beta}, \boldsymbol{\xi}_1, \dots, \boldsymbol{\xi}_p)$  is currently updated in one large block via adaptive Metropolis. For this reason, the full Bayesian P-spline approach may be a better choice, but requires updating high-dimensional vectors of spline coefficient parameters, and their suggested iteratively weighted least squares proposals would need to be modified to handle our survival models. We hope to include this in future updates of the R package

Bayes factors can be used to test the linearity of  $x_{ij\ell}$  through the hypothesis  $H_0 : \boldsymbol{\xi}_\ell = \mathbf{0}$  versus  $H_1 : \boldsymbol{\xi}_\ell \neq \mathbf{0}$ . Let  $BF_{10}$  be the Bayes factor between  $H_1$  and  $H_0$ . We estimate  $BF_{10}$  by a large-sample approximation to the Savage-Dickey density ratio (Dickey, 1971)

$$\widehat{BF}_{10} = \frac{N_K(\mathbf{0}; \mathbf{0}, gn(\mathbf{X}'_\ell \mathbf{X}_\ell)^{-1})}{N_K(\mathbf{0}; \hat{\mathbf{m}}_\ell, \hat{\boldsymbol{\Sigma}}_\ell)}, \quad (\text{G.11})$$

where  $\hat{\mathbf{m}}_\ell$  and  $\hat{\boldsymbol{\Sigma}}_\ell$  are posterior mean and covariance of  $\boldsymbol{\xi}_\ell$ .

## Appendix H Implementation Using R

An illustrative use of the R function `survregbayes` in the package `spBayesSurv` is presented to fit AFT, PH and PO frailty models with the TBP prior on baseline survival functions using simulated data. We take Example 2 of the variable selection simulation (see **Simulation IV** below) as an example. The following code is used to generate data:

```
##-----Load libraries-----##
rm(list=ls())
library(coda)
library(survival)
library(spBayesSurv)
library(BayesX)

##-----Set the true models-----##
betaT = c(1,1,0,0,0);
## Baseline Survival
f0oft = function(t) 0.5*dlnorm(t, -1, 0.5)+0.5*dlnorm(t,1,0.5);
S0oft = function(t) 0.5*plnorm(t, -1, 0.5, lower.tail=FALSE)+
0.5*plnorm(t, 1, 0.5, lower.tail=FALSE)
## The Survival function:
Sioft = function(t,x,v=0) exp( log(S0oft(t))*exp(sum(x*betaT)+v) ) ;
Fioft = function(t,x,v=0) 1-Sioft(t,x,v);
## The inverse for Fioft
Finv = function(u, x,v=0) uniroot(function (t) Fioft(t,x,v)-u, lower=1e-100, upper=1e100,
extendInt ="yes")$root

##-----Generate data-----##
## read the adjacency matrix of Nigeria for the 37 states
nigeria=read(system.file("otherdata/nigeria.bnd",
package="spBayesSurv"));
adj.mat=bnd2gra(nigeria)
W = diag(diag(adj.mat)) - as.matrix(adj.mat); m=nrow(W);
tau2T = 1;
covT = tau2T*solve(diag(rowSums(W))-W+diag(rep(1e-10, m)));
```

```

v0 = MASS::mvrnorm(n=1, mu=rep(0,m), Sigma=covT);
v = v0-mean(v0);
mis = rep(20, m); n = sum(mis);
vn = rep(v, mis);
id = rep(1:m, mis);
## generate x
x1 = rbinom(n, 1, 0.5); x2 = rnorm(n, 0, 1);
x3 = x2+0.15*rnorm(n); x4 = rnorm(n, 0, 1); x5 = rnorm(n, 0, 1);
X = cbind(x1, x2, x3, x4, x5);
colnames(X) = c("x1", "x2", "x3", "x4", "x5");
## generate survival times
u = runif(n);
tT = rep(0, n);
for (i in 1:n){
tT[i] = Finv(u[i], X[i,], vn[i]);
}
## generate partly interval-censored data
t1=rep(NA, n);t2=rep(NA, n); delta=rep(NA, n);
n1 = floor(0.5*n); ## right-censored part
n2 = n-n1; ## interval-censored part
# right-censored part
rcen = sample(1:n, n1);
t1_r=tT[rcen];t2_r=tT[rcen];
Centime = runif(n1, 2, 6);
delta_r = (tT[rcen]<=Centime) +0 ; length(which(delta_r==0))/n1;
t1_r[which(delta_r==0)] = Centime[which(delta_r==0)];
t2_r[which(delta_r==0)] = NA;
t1[rcen]=t1_r; t2[rcen]=t2_r; delta[rcen] = delta_r;
# interval-censored part
intcen = (1:n)[-rcen];
t1_int=rep(NA, n2);t2_int=rep(NA, n2); delta_int=rep(NA, n2);
npois = rpois(n2, 2)+1;
for(i in 1:n2){
gaptime = cumsum(rexp(npois[i], 1));
pp = Fioft(gaptime, X[intcen[i],], vn[intcen[i]]);
ind = sum(u[intcen[i]]>pp);
if (ind==0){
delta_int[i] = 2;
t2_int[i] = gaptime[1];
}else if (ind==npois[i]){
delta_int[i] = 0;
t1_int[i] = gaptime[ind];
}else{
delta_int[i] = 3;
t1_int[i] = gaptime[ind];
t2_int[i] = gaptime[ind+1];
}
}
t1[intcen]=t1_int; t2[intcen]=t2_int; delta[intcen] = delta_int;
## make a data frame
d = data.frame(t1=t1, t2=t2, X, delta=delta, tT=tT, ID=id, frail=vn); table(d$delta)/n;

##----- Fit the PH model with variable selection -----##
# MCMC parameters
nburn=10000; nsave=2000; nskip=4; niter = nburn+nsave
mcmc=list(nburn=nburn, nsave=nsave, nskip=nskip, ndisplay=500);
prior = list(maxL=15, a0=1, b0=1);
state <- list(cpar=1);
ptm<-proc.time()

```

```

res2 = survregbayes(formula = Surv(t1, t2, type="interval2")~x1+x2+x3+
x4+x5+frailtyprior("car", ID),
data=d, survmodel="PH", selection=TRUE, prior=prior, mcmc=mcmc, state=state,
dist="loglogistic", Proximity = W);
sfit2=summary(res2); sfit2;
systime2=proc.time()-ptm; systime2;

```

Note that the data have to be sorted by region ID before model fitting. The argument `mcmc` above specifies that the chain is subsampled every 5 iterates to get a total of 2,000 scans after a burn-in period of 10,000 iterations. The argument `prior` is used set all the priors; if nothing is specified, the default priors in the paper are used. The output is given below:

Posterior inference of regression coefficients

(Adaptive M-H acceptance rate: 0.105):

	Mean	Median	Std. Dev.	95%CI-Low	95%CI-Upp
x1	1.00002	1.00201	0.09491	0.82401	1.18337
x2	0.93568	0.97427	0.16605	0.44710	1.15790
x3	-0.68349	-0.66875	0.83818	-2.26155	0.56054
x4	0.03566	0.06164	0.75003	-1.42845	1.47316
x5	-0.02822	0.01343	0.72955	-1.43050	1.28246

Posterior inference of precision parameter

(Adaptive M-H acceptance rate: 0.2652):

	Mean	Median	Std. Dev.	95%CI-Low	95%CI-Upp
alpha	0.3843	0.3642	0.1509	0.1541	0.7288

Posterior inference of conditional CAR frailty variance

	Mean	Median	Std. Dev.	95%CI-Low	95%CI-Upp
variance	0.6576	0.6162	0.2504	0.2994	1.2456

Variable selection:

	x1,x2	x1,x2,x3	x1,x2,x4	x1,x2,x5	x1,x2,x3,x5	x1,x2,x3,x4	x1,x2,x4,x5
prop.	0.6490	0.2245	0.0505	0.0485	0.0155	0.0075	0.0045

Log pseudo marginal likelihood: LPML=-417.0232

Deviance Information Criterion: DIC=833.0498

Number of subjects: n=740

**Remarks:** The function `survregbayes` can also fit a semiparametric survival model (AFT, PH, or PO) with independent Gaussian frailties by setting `frailtyprior("iid", ID)`, with Gaussian random field frailties by setting `frailtyprior("grf", ID)`, a model without frailties by removing `frailtyprior()` in the formula, and a parametric (loglogistic, lognormal or weibull) survival model by specifying `a0` at a negative value and adding an argument `state=list(cpar=Inf)`. If FSA is used for GRF frailty models, the number of knots  $A$  and the number of blocks  $B$  are specified via `prior=list(nknots=A, nblock=B)`.

## Appendix I Additional Results for Real Data Applications

### I.1 Loblolly Pine Survival Data

Table S3 presents some baseline characteristics for the trees.



Table S3: Loblolly pine data. Baseline characteristics of the 45,525 trees.

Categorical variables	Level	Proportion (%)
Censoring status	uncensored	12.65
	right censored	87.35
Treatment (treat)	1-control	24.78
	2-light thinning	40.32
	3-heavy thinning	34.90
Physiographic region (PhyReg)	1-coastal	55.53
	2-piedmont	37.01
	3-other	7.46
Crown class (C)	1-dominant	28.21
	2-codominant	52.22
	3-intermediate	15.50
	4-suppressed	4.07
Continuous variables	Mean	Std. Dev.
Total height of tree in meters (TH)	38.47	11.77
Diameter at breast height in cm (DBH)	5.88	1.77

## Appendix J Additional Results for Simulations

### J.1 Simulation I: Areal Data

Figure S1 presents the average, across the 500 MC replicates, of fitted (posterior means over a grid of time points) baseline survival functions; the proposed method capably captures complex (here bimodal) baseline survival curves.

### J.2 Simulation III: Georeferenced Data

We generated the data using the same settings as **Simulation I** except that  $i = 1, \dots, 150, j = 1, \dots, 5$ , and  $v_i$  follows the GRF prior with  $\tau^2 = 1, \nu = 1$  and  $\phi = 1$ . The locations  $\{\mathbf{s}_i\}_{i=1}^{150}$  were generated from  $[0, 10]^2$  uniformly. Table S4 summaries the results, where we see that the point estimates of  $\beta$  are unbiased under all three models, SD-Est values are close to the corresponding PSDs, and the CP values are close to the nominal 95% level. We also observe that  $\phi$  tends to be overestimated and the standard deviations for  $\tau^2$  and  $\phi$  are underestimated (because SD-Est is smaller than PSD). Even though, the CP values are still close to 95%. The ESS values for  $\beta$  are much smaller than these obtained for areal data, indicating that the georeferenced spatial dependency makes the posterior samples more correlated.

### J.3 Simulation IV: Variable Selection

We next assess the performance of our variable selection method via three simulated examples. For each example, one data set was generated from the PH model with  $S_0(t)$  and ICAR as in **Simulation I**. Under Example 1, we set  $\mathbf{x}_{ij} = (x_{ij1}, \dots, x_{ij5})$  with  $x_{ij1} \sim \text{Bernoulli}(0.5)$  and  $x_{ij2}, \dots, x_{ij5} \stackrel{iid}{\sim} N(0, 1)$ , and  $\beta = (1, 1, 0, 0, 0)'$ . Example 2 is identical to Example 1 except that  $x_{ij3} = x_{ij2} + 0.15z$  where  $z \sim N(0, 1)$ , yielding a 0.989 correlation between  $x_2$  and  $x_3$ . For Example 3, we set  $\mathbf{x}_{ij} = (x_{ij1}, \dots, x_{ij10})$  with  $\beta = (1, 1, 1, 1, 1, 0, 0, 0, 0, 0)$  and  $x_{ijk}|z \stackrel{iid}{\sim} N(z, 1)$  where

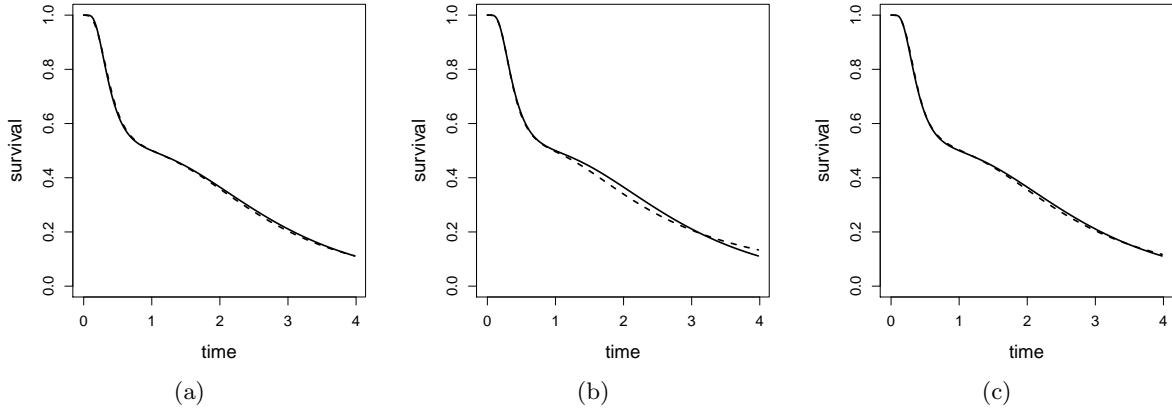


Figure S1: Simulated I. Mean, across the 500 MC replicates, of the posterior mean of the baseline survival functions under AFT (panel a), PH (panel b) and PO (panel c). The true curves are represented by continuous lines and the fitted curves are represented by dashed lines.

Table S4: Simulation III. Averaged bias (BIAS) and posterior standard deviation (PSD) of each point estimate, standard deviation (across 500 MC replicates) of the point estimate (SD-Est), coverage probability (CP) for the 95% credible interval, and effective sample size (ESS) for each point estimate.

Model	Parameter	BIAS	PSD	SD-Est	CP	ESS
AFT	$\beta_1 = 1$	-0.002	0.085	0.089	0.946	1933
	$\beta_2 = 1$	-0.000	0.045	0.042	0.964	1815
	$\tau^2 = 1$	0.000	0.329	0.220	0.948	548
	$\phi = 1$	0.082	0.388	0.357	0.962	471
PH	$\beta_1 = 1$	-0.016	0.112	0.116	0.934	1943
	$\beta_2 = 1$	-0.015	0.068	0.068	0.942	1110
	$\tau^2 = 1$	0.042	0.451	0.316	0.938	366
	$\phi = 1$	0.066	0.471	0.420	0.918	351
PO	$\beta_1 = 1$	-0.001	0.157	0.159	0.952	3006
	$\beta_2 = 1$	0.003	0.087	0.088	0.944	1960
	$\tau^2 = 1$	0.034	0.410	0.341	0.954	502
	$\phi = 1$	0.313	1.361	0.768	0.912	353

Table S5: Simulated IV. High frequency models with selected variables.

Example 1		Example 2		Example 3	
Variables	Proportions	Variables	Proportions	Variables	Proportions
1 2	0.80	1 2	0.49	1-5	0.63
1 2 3	0.08	1 2 3	0.22	1-5, 10	0.15
1 2 5	0.05	1 3	0.17	1-5, 7	0.09
1 2 4	0.05	1 2 5	0.04	1-5, 8	0.05

$z \sim N(0, 1)$ , which induces pairwise correlations of about 0.5. We applied our method to the three simulated datasets using all default priors designed for variable selection. A sample of 10,000 scans was thinned from 50,000 after a burn-in period of 10,000 iterations. Table S5 lists the proportions for the four highest frequency models under each example. The results reveal that our method predicts the right model very well even in the presence of extreme collinearity.

#### J.4 Comparing with Polya Trees

Zhao et al. (2009) considered the AFT, PH and PO models for right censored areal data, and used the mixture of Polya trees (MPT) prior on the baseline survival function. In their MCMC scheme, most parameters were updated using simple random walk Metropolis-Hastings steps, so a careful tuning of the proposal distribution was required to achieve desirable acceptance rate. We instead used adaptive Metropolis samplers (Haario et al., 2001) on most parameters and implemented the three MPT models into an R function `survregbayes2`; this function can also fit arbitrarily censored data. We generated data using the same settings as **Simulation I**, then fitted each model with finite Polya tree level equal to 4, a  $\Gamma(5, 1)$  prior on the Polya tree precision parameter, and priors on other parameters similar to Section 2.3 in the main paper. For each MCMC algorithm, 5,000 scans were thinned from 50,000 after a burn-in period of 10,000 iterations.

Table S6 summarizes the results for regression parameters  $\beta$  and the ICAR variance  $\tau^2$ , including the averaged bias (BIAS) and posterior standard deviation (PSD) of each point estimate (posterior mean for  $\beta$  and median for  $\tau^2$ ), the standard deviation (across 500 MC replicates) of the point estimate (SD-Est), the coverage probability (CP) of the 95% creditable interval, and effective sample size (ESS) out of 5,000 (Sargent et al., 2000) for each point estimate. We can see that effective sample sizes for  $\beta_1$  and  $\beta_2$  under the MPT AFT are 2 times smaller than those under the TBP AFT. In addition, the MPT PH model provides more biased estimates than the TBP PH.

Due to the non-smoothness of Polya tree densities, the MPT AFT often suffers poor mixing when the true baseline survival function is far away from the centering parametric distribution family  $S_{\theta}$  and uncensored survival times are available. For example, for right censored data, the likelihood will involve  $f_{\mathbf{x}_{ij}}(t) = e^{\mathbf{x}'_{ij}\beta + v_i} f_0(e^{\mathbf{x}'_{ij}\beta + v_i} t)$ , where  $f_0(\cdot)$  is the density of a Polya tree. Note that  $f_0(\cdot)$  consists of many big jumps when the precision parameter of the Polya trees is small, and hence a tiny change in  $\beta$  imply a big jump in the likelihood value, leading to poor mixing. However, MCMC mixing issues are mitigated for interval censored data, since only the survival function  $S_0(e^{\mathbf{x}'_{ij}\beta + v_i} t)$  is involved in the likelihood and  $S_0(t)$  is continuous.

#### J.5 Model Selection via LPML and DIC

We next demonstrate via simulations that the LPML and DIC are reasonable criteria for model selection among AFT, PH and PO models. Arbitrarily censored survival data of size  $n = 740$  and  $n = 1850$  were generated from each of the three models with ICAR frailties using the same settings

Table S6: Simulation under MPT. Averaged bias (BIAS) and posterior standard deviation (PSD) of each point estimate, standard deviation (across 500 MC replicates) of the point estimate (SD-Est), coverage probability (CP) for the 95% credible interval, and effective sample size (ESS) out of 5,000 with thinning=10 for each point estimate.

Model	Parameter	BIAS	PSD	SD-Est	CP	ESS
AFT	$\beta_1 = 1$	0.002	0.094	0.071	0.986	1009
	$\beta_2 = 1$	0.002	0.050	0.038	0.988	1079
	$\tau^2 = 1$	0.013	0.309	0.243	0.976	3760
PH	$\beta_1 = 1$	-0.045	0.099	0.098	0.932	2887
	$\beta_2 = 1$	-0.043	0.060	0.060	0.874	1794
	$\tau^2 = 1$	-0.084	0.318	0.280	0.954	3599
PO	$\beta_1 = 1$	-0.014	0.149	0.142	0.962	3579
	$\beta_2 = 1$	-0.029	0.082	0.078	0.938	2561
	$\tau^2 = 1$	-0.038	0.407	0.346	0.966	2903

as **Simulation I**. For each model, 200 MC replicates were generated. We fitted each dataset using all three models with the default priors and the same MCMC settings as **Simulation I**. Table S7 (under log-logistic  $S_{\theta}(\cdot)$ ) presents the proportion (out of 200 MC replicates) of times each model is picked. The model picked is the one with largest LPML or smallest DIC. DIC and LPML yield very similar proportions for  $n = 740$  and identical results when  $n = 1850$ , indicating that the two criteria are consistent for model comparison. When the true model is PH, DIC has a 3% chance of picking PO under  $n = 740$ , but is reduced to zero for the larger sample size  $n = 1850$ .

Table S7: Simulation for model selection via LPML and DIC. Proportion of times DIC or LPML selects each model when truth is known out of 200 replicated datasets.

True model	Criteria	log-logistic Model picked			Weibull Model picked			log-normal Model picked		
		AFT	PH	PO	AFT	PH	PO	AFT	PH	PO
$n = 740$										
AFT	DIC	1.000	0.000	0.000	1.000	0.000	0.000	1.000	0.000	0.000
	LPML	1.000	0.000	0.000	1.000	0.000	0.000	1.000	0.000	0.000
PH	DIC	0.000	0.985	0.015	0.000	1.000	0.000	0.000	1.000	0.000
	LPML	0.000	0.970	0.030	0.000	1.000	0.000	0.000	0.995	0.005
PO	DIC	0.000	0.000	1.000	0.000	0.075	0.925	0.000	0.000	1.000
	LPML	0.000	0.000	1.000	0.000	0.025	0.975	0.000	0.000	1.000
$n = 1850$										
AFT	DIC	1.000	0.000	0.000	1.000	0.000	0.000	1.000	0.000	0.000
	LPML	1.000	0.000	0.000	1.000	0.000	0.000	1.000	0.000	0.000
PH	DIC	0.000	1.000	0.000	0.000	1.000	0.000	0.000	1.000	0.000
	LPML	0.000	1.000	0.000	0.000	1.000	0.000	0.000	1.000	0.000
PO	DIC	0.000	0.000	1.000	0.000	0.010	0.990	0.000	0.000	1.000
	LPML	0.000	0.000	1.000	0.000	0.010	0.990	0.000	0.000	1.000

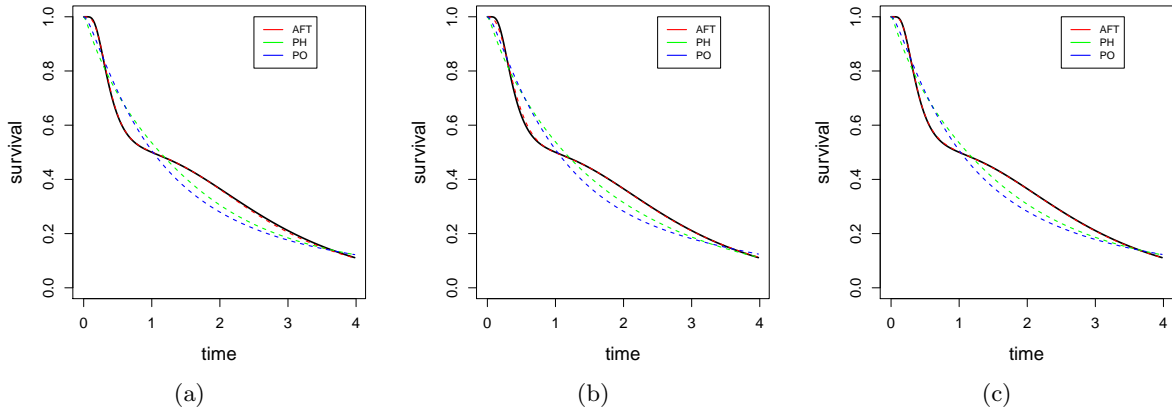


Figure S2: Simulation for sensitivity analysis of the TBP’s centering distribution when AFT is the true model. Mean, across the 200 MC replicates, of the posterior mean of the baseline survival functions under log-logistic (panel a), Weibull (panel b) and log-normal (panel c). The true curves are represented by continuous lines and the fitted curves are represented by dashed lines (red is for AFT, green is for PH and blue is for PO).

## J.6 Sensitivity Analysis of The TBP’s Centering Distribution

The TBP prior is centered at a parametric family of distributions. The log-logistic  $S_{\theta}(t) = \{1 + (e^{\theta_1}t)^{\exp(\theta_2)}\}^{-1}$ , the log-normal  $S_{\theta}(t) = 1 - \Phi\{(\log t + \theta_1) \exp(\theta_2)\}$ , and the Weibull  $S_{\theta}(t) = 1 - \exp\{- (e^{\theta_1}t)^{\exp(\theta_2)}\}$  families are implemented in the software. We next demonstrate via simulations that posterior inference and model selection is not very sensitive to the choice of centering parametric family. Table S7 presents the proportion (out of 200 MC replicates) of times each model is picked under all settings when data are generated as in the previous simulation J.5. When the true model is PH with  $n = 740$ , the Weibull centering distribution has a improved chance to pick the correct model than log-logistic, indicating that the Weibull slightly favors PH for this bimodal baseline  $S_0$ . As sample sizes increase, all three centering distributions give the same model selection results.

Figures S2, S3, and S4 present the averaged (across the 200 MC replicates) fitted baseline survival functions under three centering distribution families when the true model is AFT, PH and PO, respectively. Overall, the three families yield almost the same estimates regardless of what the true model is, although we do see that Weibull provides a slightly better estimate than the other two (Figure S3) when the true model is PH with the bimodal baseline  $S_0$  and PH is used to fit the model. We also compared the inference results on the coefficient estimates (not shown), which resulted in very similar biases, coverage probabilities and effective sample sizes.

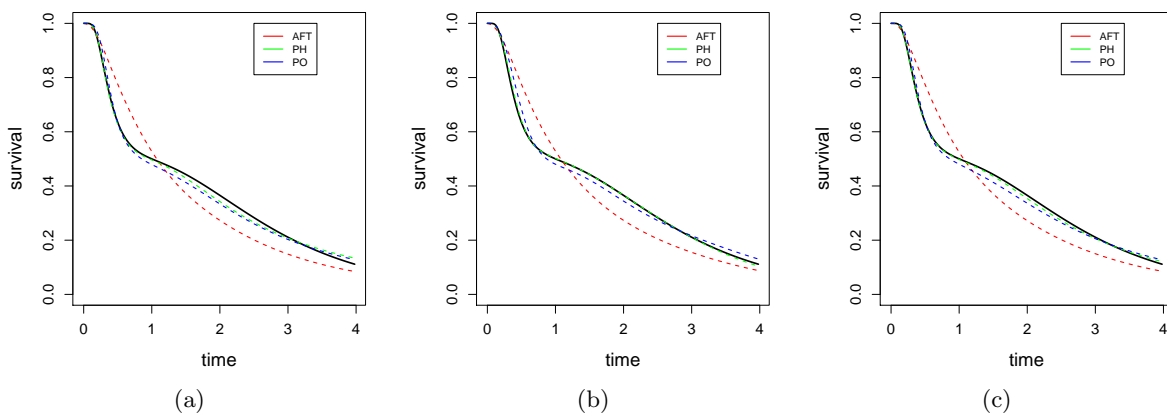


Figure S3: Simulation for sensitivity analysis of the TBP's centering distribution when PH is the true model. Mean, across the 200 MC replicates, of the posterior mean of the baseline survival functions under log-logistic (panel a), Weibull (panel b) and log-normal (panel c). The true curves are represented by continuous lines and the fitted curves are represented by dashed lines (red is for AFT, green is for PH and blue is for PO).

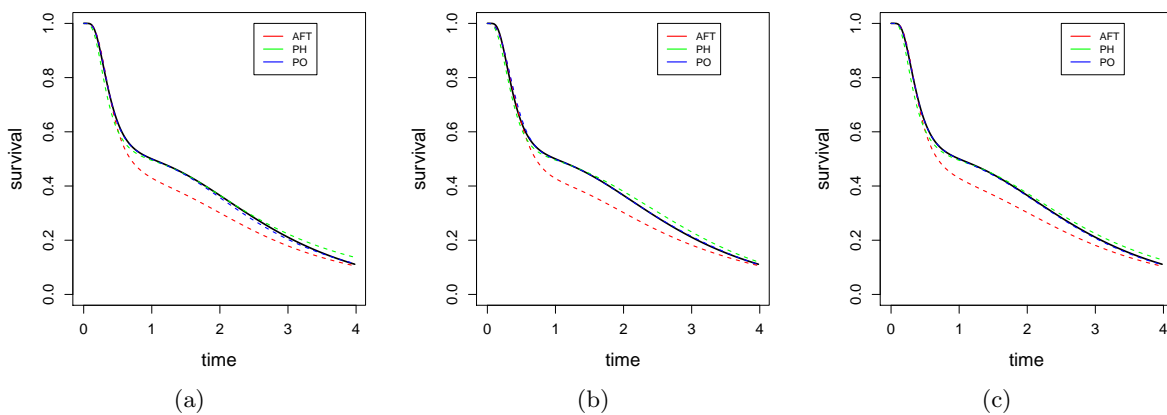


Figure S4: Simulation for sensitivity analysis of the TBP's centering distribution when PO is the true model. Mean, across the 200 MC replicates, of the posterior mean of the baseline survival functions under log-logistic (panel a), Weibull (panel b) and log-normal (panel c). The true curves are represented by continuous lines and the fitted curves are represented by dashed lines (red is for AFT, green is for PH and blue is for PO).

## References

- Banerjee, S., Carlin, B. P., and Gelfand, A. E. (2014). *Hierarchical Modeling and Analysis for Spatial Data, Second Edition*. Chapman and Hall/CRC Press.
- Bové, D. S., Held, L., et al. (2011). Hyper- $g$  priors for generalized linear models. *Bayesian Analysis*, 6(3):387–410.
- Cox, D. R. (1972). Regression models and life-tables (with discussion). *Journal of the Royal Statistical Society. Series B (Methodological)*, 34(2):187–220.
- Cox, D. R. and Oakes, D. (1984). *Analysis of Survival Data*. Chapman & Hall: London.
- Dickey, J. M. (1971). The weighted likelihood ratio, linear hypotheses on normal location parameters. *The Annals of Mathematical Statistics*, 42(1):204–223.
- Epifani, I., MacEachern, S. N., and Peruggia, M. (2008). Case-deletion importance sampling estimators: Central limit theorems and related results. *Electronic Journal of Statistics*, 2:774–806.
- Finley, A. O., Sang, H., Banerjee, S., and Gelfand, A. E. (2009). Improving the performance of predictive process modeling for large datasets. *Computational Statistics & Data Analysis*, 53(8):2873–2884.
- Geisser, S. and Eddy, W. F. (1979). A predictive approach to model selection. *Journal of the American Statistical Association*, 74(365):153–160.
- Gelfand, A. E. and Dey, D. K. (1994). Bayesian model choice: Asymptotics and exact calculations. *Journal of the Royal Statistical Society: Series B*, 56(3):501–514.
- Gelman, A., Hwang, J., and Vehtari, A. (2014). Understanding predictive information criteria for Bayesian models. *Statistics and Computing*, 24(6):997–1016.
- George, E. I. and McCulloch, R. E. (1993). Variable selection via Gibbs sampling. *Journal of the American Statistical Association*, 88(423):881–889.
- Gray, R. J. (1992). Flexible methods for analyzing survival data using splines, with applications to breast cancer prognosis. *Journal of the American Statistical Association*, 87(420):942–951.
- Haario, H., Saksman, E., and Tamminen, J. (2001). An adaptive Metropolis algorithm. *Bernoulli*, 7(2):223–242.
- Han, C. and Carlin, B. P. (2001). Markov chain Monte Carlo methods for computing Bayes factors. *Journal of the American Statistical Association*, 96(455):1122–1132.
- Hanson, T., Johnson, W., and Laud, P. (2009). Semiparametric inference for survival models with step process covariates. *Canadian Journal of Statistics*, 37(1):60–79.
- Hanson, T. E., Branscum, A. J., and Johnson, W. O. (2014). Informative  $g$ -priors for logistic regression. *Bayesian Analysis*, 9(3):597–612.
- Hennerfeind, A., Brezger, A., and Fahrmeir, L. (2006). Geoaddivitive survival models. *Journal of the American Statistical Association*, 101(475):1065–1075.

- Ibrahim, J. G., Chen, M.-H., and Sinha, D. (2001). Criterion-based methods for Bayesian model assessment. *Statistica Sinica*, 11(2):419–443.
- Johnson, M. E., Moore, L. M., and Ylvisaker, D. (1990). Minimax and maximin distance designs. *Journal of Statistical Planning and Inference*, 26(2):131–148.
- Kass, R. E. and Raftery, A. E. (1995). Bayes factors. *Journal of the American Statistical Association*, 90(430):773–795.
- Kneib, T. (2006). Mixed model-based inference in geoadditive hazard regression for interval-censored survival times. *Computational Statistics & Data Analysis*, 51(2):777–792.
- Konomi, B. A., Sang, H., and Mallick, B. K. (2014). Adaptive Bayesian nonstationary modeling for large spatial datasets using covariance approximations. *Journal of Computational and Graphical Statistics*, 23(3):802–929.
- Kuo, L. and Mallick, B. (1998). Variable selection for regression models. *Sankhyā: The Indian Journal of Statistics, Series B*, 60(1):65–81.
- Lang, S. and Brezger, A. (2004). Bayesian p-splines. *Journal of Computational and Graphical Statistics*, 13(1):183–212.
- Nardi, A. and Schemper, M. (2003). Comparing Cox and parametric models in clinical studies. *Statistics in Medicine*, 22(23):3597–3610.
- O’Hara, R. B. and Sillanpää, M. J. (2009). A review of Bayesian variable selection methods: What, how and which. *Bayesian Analysis*, 4(1):85–118.
- Pavlou, M., Ambler, G., Seaman, S., De Iorio, M., and Omar, R. Z. (2016). Review and evaluation of penalised regression methods for risk prediction in low-dimensional data with few events. *Statistics in Medicine*, 35(7):1159–1177.
- Prentice, R. L. and Kalbfleisch, J. D. (1979). Hazard rate models with covariates. *Biometrics*, 35(1):25–39.
- Sang, H. and Huang, J. Z. (2012). A full scale approximation of covariance functions for large spatial data sets. *Journal of the Royal Statistical Society: Series B (Statistical Methodology)*, 74(1):111–132.
- Sargent, D. J., Hodges, J. S., and Carlin, B. P. (2000). Structured Markov chain Monte Carlo. *Journal of Computational and Graphical Statistics*, 9(2):217–234.
- Vehtari, A. and Gelman, A. (2014). *WAIC and cross-validation in Stan*. [http://www.stat.columbia.edu/~gelman/research/unpublished/waic\\_stan.pdf](http://www.stat.columbia.edu/~gelman/research/unpublished/waic_stan.pdf).
- Vehtari, A., Gelman, A., and Gabry, J. (2017). Practical Bayesian model evaluation using leave-one-out cross-validation and WAIC. *Statistics and Computing*, 27(5):1413–1432.
- Verdinelli, I. and Wasserman, L. (1995). Computing Bayes factors using a generalization of the Savage-Dickey density ratio. *Journal of the American Statistical Association*, 90(430):614–618.
- Watanabe, S. (2010). Asymptotic equivalence of Bayes cross validation and widely applicable information criterion in singular learning theory. *Journal of Machine Learning Research*, 11(Dec):3571–3594.



- Zellner, A. (1983). Applications of Bayesian analysis in econometrics. *The Statistician*, 32:23–34.
- Zhao, L., Hanson, T. E., and Carlin, B. P. (2009). Mixtures of Polya trees for flexible spatial frailty survival modelling. *Biometrika*, 96(2):263–276.
- Zhou, H., Hanson, T., and Zhang, J. (2017). Generalized accelerated failure time spatial frailty model for arbitrarily censored data. *Lifetime Data Analysis*, 23(3):495–515.